Published online 4 March 2016

Nucleic Acids Research, 2016, Vol. 44, No. 11 ***5105–5122***
doi: 10.1093/nar/gkw113

Bidirectional promoters link cAMP signaling with irreversible differentiation through promoter-associated non-coding RNA (pancRNA) expression in PC12 cells

Naoki Yamamoto[1,2], Kiyokazu Agata[2], Kinichi Nakashima[1] and Takuya Imamura[1,*]

[1]Department of Stem Cell Biology and Medicine, Graduate School of Medical Sciences, Kyushu University, Japan and [2]Department of Biophysics, Graduate School of Science, Kyoto University, Japan

Received November 18, 2015; Revised January 25, 2016; Accepted February 16, 2016

ABSTRACT

Bidirectional promoters are the major source of gene activation-associated noncoding RNA (ncRNA). PC12 cells offer an interesting model for understanding the mechanism underlying bidirectional promoter-mediated cell cycle control. Nerve growth factor (NGF)-stimulated PC12 cells elongate neurites, and are in a reversible cell-cycle-arrested state. In contrast, these cells irreversibly differentiate and cannot re-enter the normal cell cycle after NGF plus cAMP treatment. In this study, using directional RNA-seq, we found that bidirectional promoters for protein-coding genes with promoter-associated ncRNA (pancRNA) were enriched for cAMP response element consensus sequences, and were preferred targets for transcriptional regulation by the transcription factors in the cAMP-dependent pathway. A spindle-formation-associated gene, *Nusap1* and *pancNusap1* were among the most strictly co-transcribed pancRNA–mRNA pairs. This pancRNA–mRNA pair was specifically repressed in irreversibly differentiated PC12 cells. Knockdown (KD) and overexpression experiments showed that *pancNusap1* positively regulated the *Nusap1* expression in a sequence-specific manner, which was accompanied by histone acetylation at the *Nusap1* promoter. Furthermore, *pancNusap1* KD recapitulated the effects of cAMP on cell cycle arrest. Thus, we conclude that pancRNA-mediated histone acetylation contributes to the establishment of the cAMP-induced transcription state of the *Nusap1* locus and contributes to the irreversible cell cycle exit for terminal differentiation of PC12 cells.

INTRODUCTION

Many long noncoding RNAs (lncRNAs) have been shown to be transcribed from the mammalian genome, and have emerged as key players of many cellular functions (1–4). The majority of non-coding RNAs (ncRNAs) involved in mRNA metabolism in mammals have been thought to downregulate the corresponding mRNA expression level in a pre- or post-transcriptional manner by forming ncRNA–mRNA duplex structures (2,5). However, several studies have shown that some lncRNAs function without forming RNA–RNA duplexes (6–9).

The transcripts derived from bidirectional promoters include not only protein-coding mRNAs, but also lncRNAs, and a significant proportion of such lncRNAs derived from bidirectional promoters are expressed in tissue-specific manners (10,11). We previously showed that functional polyA+, long (>200 bp) ncRNAs derived from bidirectional promoters, named promoter-associated ncRNAs (pancRNAs), are expressed in tissue-specific manners and function in the activation of their partner genes (7,8,11,12). For example, in mice, microinjection of siRNA against the abundant pancRNA partner of interleukin 17d (*Il17d*) mRNA at the 1-cell stage caused embryonic lethality, which was rescued by supplying IL17D protein *in vitro* at the 4-cell stage (7). Thousands of pancRNAs are generated by transcription of the antisense strand and exhibit expression changes coordinated with the expression of their cognate genes (11), making bidirectional promoters a major source of gene activation-associated ncRNA.

Transcriptional regulation by binding of transcription factors to the cAMP response element (CRE) downstream of cAMP signaling plays important roles in the cell differentiation process (13,14). Transcription factors that bind to CRE, such as CRE-binding protein (Creb) and CRE modulator (Crem), are activated by cAMP-dependent protein kinase (Pka)-mediated phosphorylation, and activate

*To whom correspondence should be addressed. Tel: +81 92 642 6196; Fax: +81 92 642 6561; Email: imamura@scb.med.kyushu-u.ac.jp
Present address: Naoki Yamamoto, Life Science Tokyo Advanced Research center (L-StaR), Hoshi University School of Pharmacy and Pharmaceutical Science, Japan.

gene expression by means of recruitment of coactivator paralogs CREB-binding protein (Cbp) and p300 (15,16). Transcription factors that bind to CRE can act not only as transcriptional activators but also as transcriptional repressors. Inducible cAMP early repressor (Icer) is generated from an alternative intronic promoter of *Crem*, and acts as a transcriptional repressor (17). Icer lacks the activation and kinase-inducible domains, but retains the DNA-binding domain (18,19), and therefore is a potent repressor of cAMP-induced transcription. In a different context, CREB1 forms a complex with p53, and then inhibits p53-mediated transcriptional activation of the MDM2 gene in a human cell line during glucose deprivation (20). It is noteworthy that, using chromatin immunoprecipitation (ChIP) coupled with massively parallel sequencing (ChIP-seq), Impey *et al*. demonstrated that phosphorylated Creb1 (pCreb1)-bound regions are enriched in the bidirectional promoters of annotated transcript pairs that are organized in a head-to-head arrangement on opposite strands (15). Thus, comprehensive analysis of bidirectional promoters may identify a set of transcripts that are upregulated and downregulated by cAMP and that play a role in defining the cell state. We hypothesize that certain pancRNAs derived from bidirectional promoters are upregulated or downregulated by a cAMP-dependent mechanism.

In this context, rat adrenal phaeochromocytoma-derived PC12 cells offer an interesting model for studying cAMP-dependent pancRNA functions in cell cycle regulation associated with differentiation. Nerve growth factor (NGF)-stimulated PC12 cells elongate neurites and are reversibly arrested, that is, they can resume efficient cell cycling when they are put back under proliferative conditions (21). In contrast, when PC12 cells are stimulated simultaneously with NGF and a cAMP analog, dibutyryl cAMP (db-cAMP), they cannot re-enter the cell cycle even after the removal of NGF and dbcAMP (22). This shows that irreversible differentiation of PC12 cells can be induced by a cAMP-dependent mechanism. A previous *in vivo* study showed that pharmacological activation of the cAMP pathway rescued impairment of neuronal differentiation of neural progenitors caused by brain-specific knockout of the *Nf1* gene in mice, suggesting that a cAMP-dependent mechanism is also required for the *in vivo* neuronal differentiation of neural progenitor cells (13). The cell cycle of terminally differentiated cells is repressed by a cAMP-dependent mechanism, but the underlying molecular mechanisms are unknown.

In this study, by comparing the transcriptome of NGF-differentiated (Ndiff) PC12 cells with that of NGF/cAMP-differentiated (NcAdiff) PC12 cells, we highlighted the critical importance of cell cycle regulation for the terminal differentiation of cells that cannot resume mitosis. We showed that a significant number of M-phase-associated genes were repressed in NcAdiff cells, compared to Ndiff cells. As expected, we found that a significant number of CREs were enriched in the thousands of newly identified bidirectional promoters for the expression of pancRNA–mRNA pairs. Here, we report that these bidirectional promoters were preferred targets for transcriptional regulation by the transcription factors in the cAMP-dependent pathway. Furthermore, among the pancRNA–mRNA pairs, a pancRNA (*pancNusap1*) at the *Nusap1* locus, which encodes a spindle-formation-associated gene, and *Nusap1* mRNA together play a functional role in the irreversible differentiation of PC12 cells. Artificial downregulation of the *pancNusap1* expression level recapitulated the cAMP-triggered morphological features and epigenetic state of the irreversibly differentiated PC12 cells.

MATERIALS AND METHODS

PC12 culture and differentiation

PC12 cells were maintained in high-glucose Dulbecco's modified Eagle's medium (DMEM) (WAKO) containing 10% horse serum (HS; SAFC Biosciences), 5% fetal bovine serum (FBS; Biowest), 100 units/ml penicillin (PhytoTechnology Laboratories), and 100 μg/ml streptomycin (MP Biomedicals) at 37°C in 5% CO_2. To induce differentiation, PC12 cells were placed on a collagen (Cellmatrix Type IV, Nitta Gelatin)-precoated dish at a density of 8000 cells/cm^2, and were cultured in high-glucose DMEM containing 1% HS, 0.5% FBS, 100 units/ml penicillin, 100 μg/ml streptomycin, 100 ng/ml NGF 2.5S (Millipore) or 50 ng/ml NGF 2.5S and 200 μM dibutyryl cAMP (SIGMA) for 7 days. During differentiation, cell culture medium was changed at day 3 and day 5. To observe the cell cycle resumption of differentiated PC12 cells, the differentiation medium was changed at day 7 to high-glucose DMEM containing 10% HS, 5% FBS and antibiotics. For doxycycline (Dox)-inducible pancRNA overexpression/knockdown (OE/KD) experiments, cells were incubated in the above medium containing 2 ng/ml Dox (Nacalai Tesque).

Immunocytochemistry

Immunocytochemistry was performed as follows: fixation with 4% paraformaldehyde (PFA) for 20 min in RT; washing with phosphate buffered saline (PBS) twice; permeabilization and blocking in PBS containing 0.1% Triton X-100 and 3% FBS in PBS for 30 min at RT; incubation with primary antibody diluted 1:500 in blocking solution for 2 h in RT; washing with PBS three times; incubation with Hoechst 33258 (Nacalai Tesque) and secondary antibody diluted 1:500 in PBS for 1 h in the dark at RT; washing with PBS three times. Imaging was performed using a Leica AF6000 microscope. As primary antibodies, chicken anti-GFP (AVES Labs), mouse anti-Ki67 (BD Biosciences) and rabbit anti-active Caspase 3 (R&D Systems) were used. As secondary antibodies, the following were used: CF647-conjugated anti-mouse IgG (Biotium) and CF647-conjugated anti-rabbit IgG (Biotium), FITC-conjugated anti-chick IgY (Biotium). For the EdU assay, cells were cultured with 10 μM EdU in Click-iT EdU Imaging Kits (Life Technologies) for 4 h, fixed with 4% PFA, permeabilized with 0.1% Triton-X and 3% FBS in PBS, and stained with Click-iT reaction buffer for 30 min at RT in the dark. After washing with PBS, primary and secondary staining were performed in the dark.

RNA analysis

To examine RNA expression, total RNA isolated with TRIzol reagent (Life Technologies) was treated with DNase

I (Life Technologies) and reverse-transcribed with oligo dT primer using the SuperScriptIII First-Strand Synthesis System (Life Technologies). Synthesized cDNAs were subjected to qPCR using a KAPA SYBR Fast qPCR Kit (KAPA Biosystems). The primers used in these analyses are listed in Supplementary Table S1.

Directional RNA-seq library preparation

Directional RNA-seq libraries were prepared as follows. RNA with RNA integrity number above 9.6, calculated using total RNA Pico Bioanalyzer chip (Agilent), was used for Directional RNA-seq library preparation. polyA+ RNA was purified twice from 15 μg of total RNA of each PC12 sample by using Sera-mag Magnetic Oligo (dT) Beads (Thermo Scientific). In each polyA+ RNA sample, the fraction of rRNA was confirmed to be <2% by using a Total RNA Pico Bioanalyzer chip. The polyA+ RNA was fragmented by heating at 94°C for 2 min in 1 × fragmentation buffer (Affymetrix), and then the RNA was purified with two volumes of Agencourt RNAclean XP (Beckman Coulter). Fragmented RNA was decapped with 5 U TAP (Epicenter), and then subjected to phenol:chloroform:isoamylalcohol (PCI) extraction and ethanol precipitation. Fragmented and decapped RNA was 3′-dephosphorylated using Antarctic phosphatase (NEB). The RNA was 5′-phosphorylated using T4 polynucleotide kinase (NEB). The modified RNA was cleaned up with an RNeasy MinElute kit (Qiagen), was ligated to NEBNext Multiplex 3′ SR Adaptor with T4 RNA ligase 2 truncated K277Q (NEB) at 4°C overnight, and was further ligated to NEBNext Multiplex 5′ SR Adaptor with T4 RNA ligase (Illumina) at 20°C for 1 h. cDNA was synthesized with specific RT primer and the SuperScriptIII First-Strand Synthesis System. After RNase H treatment, unincorporated primers in each cDNA library sample were removed by using AMPure XP (Beckman Coulter). Each cDNA was independently amplified with KAPA Hifi HS polymerase (Kapa Biosystems) and NEBNext Index 1, 8, 10 and 11 primers in NEBNext Multiplex Oligos for Illumina (NEB) to produce four replicates for each sample. Thermal-cycling conditions were as follows: 30 s at 98°C, 12 cycles of 98°C for 15 s, 62°C for 30 s and 72°C for 30 s, followed by 5 min at 72°C. The polymerase chain reaction (PCR) product was purified twice with AMPure XP. Illumina HiSeq 2000 was used to perform 50-bp single-end sequencing according to the manufacturer's instructions.

Data mining

To remove low quality reads and adaptor sequences (AGATCGGAAGAGCACACGTCTGAACTCCAGTCAC), the FASTX tool kit (http://hannonlab.cshl.edu/fastx_toolkit/index.html) was used as follows: Remove low quality reads (phred score <20); remove 3′-end multiplex adapter tag sequence; remove the reads shorter than 20 nt; remove low quality reads again. The raw reads from all PC12 samples resulted in a total of 517 million strand-specific reads. We mapped sequencing reads from each sample onto the rat Rn5 genome sequences except for random chromosome sequences using TopHat (v.2.0.8b, option: -g 1 –bowtie1) (23). RSeQC (24) was used for quality evaluation of the strandedness in our cDNA libraries. The read-enriched regions in each cell state were detected using MACS2 (v.2.0.10b, option: –nomodel –broad -g 2.57e9 -p 0.95) (25). All reads in biological replicates were merged and used as the input data for MACS2. Overlapping read-enriched regions between different cell states were merged to create one broad region using the mergeBed function of BEDTools (26). This resulted in 149 559 read-enriched regions (minimum length set to 300 nt). When a reference transcription start site (TSS) in the Rn5 genome assembly was overlapped with a read-enriched region, we defined the 5′-end of this region as the adjusted TSS in PC12 cell samples except for cases in which the 5′-end overlapped with another gene. The coding potentials of non-annotated transcripts and candidate-pancRNAs were estimated using the coding potential calculator (CPC) algorithm (27). For mRNA and ncRNA quantification, we counted the number of reads mapped to the exonic region of Ensembl protein-coding genes and read-enriched regions classified as non-annotated transcripts, respectively, followed by normalization using the iDEGES/edgeR methods and differential expression analyses using R package TCC (28).

For the correlation analysis in Figure 3C, Pearson correlation coefficients between the expression levels of novel transcripts and annotated protein-coding genes were calculated. In this analysis, randomly selected lncRNA and mRNA pairs were generated using the publicly available program (https://cell-innovation.nig.ac.jp/wiki/tiki-download_wiki_attachment.php?attId=5&download=y). For enrichment analysis of biological process ontology, differentially expressed genes were annotated using DAVID (29).

Enrichment analysis of CRE and Creb1 binding score in bidirectional promoter

For enrichment analysis of CREs, the locations of CREs were searched using the R package ChIPpeakAnno (option: min.score = '90%') (30) using Creb1 binding sequence data that is registered in the JASPAR database (ID = MA0018.2) (31).

For enrichment analysis of Creb1 binding score, the mouse Mm9 genome-mapped Creb1 ChIP-seq dataset of E16.5 mouse cortical neurons that had been maintained *in vitro* for 7 days obtained from Gene Expression Omnibus (acc. no GSM530185) (32) was converted to the corresponding dataset in the rat Rn5 genome using the UCSC LiftOver tool (http://hgdownload.cse.ucsc.edu/admin/exe). Similarly, the rat rn3 genome-mapped pCreb1 ChIP-seq dataset of PC12 cells 15 min after cAMP signal activation by forskolin (15), deposited as a supplementary data of a serial report (33), was converted to the corresponding dataset in the rat Rn5 genome using the UCSC LiftOver tool.

Chromatin immunoprecipitation (ChIP) analysis

For ChIP analysis, we generated Dox-inducible short hairpin RNA (shRNA)-expressing or pancRNA-expressing PC12 cell lines, as described later. Cells (about 4 × 10^5) in

a 10-cm Petri dish were fixed with 1% formaldehyde for 5 min at RT. Samples were placed on ice and washed twice with ice-cold PBS. Cells were harvested by scraping with 1 ml of resuspension solution (10% NaN_3, 2% FBS in 1 × PBS) and counted, and were centrifuged at 2000 g for 5 min at 4°C. Cell pellets were washed with 1 ml of ice-cold PBS, resuspended in lysis buffer containing 1% sodium dodecyl sulphate (SDS), 50 mM Tris–HCl [pH 8.0], 10 mM ethylenediaminetetraacetic acid (EDTA) [pH 8.0] and 1% protease inhibitor cocktail (Nacalai Tesque) at a concentration of 1 × 10^5 cells per 100 μl, kept on ice for 10 min, then sonicated to an average size of 500 bp using a Bioruptor (Diagenode). After centrifugation for 15 min at 15 000 rpm at 4°C, supernatants containing sonicated chromatin were transferred to fresh tubes and diluted 1:10 with ChIP dilution buffer (1.1% Triton X-100, 50 mM Tris–HCl [pH 8.0], 167 mM NaCl, 0.11% sodium deoxycholate, 1% protease inhibitor cocktail). Immunoreaction was performed overnight at 4°C with rotation. For each sample preparation, 5 × 10^4 cells and 1 μl of each antibody (anti-mouse-H3K4me3, anti-mouse-H3K9me3, anti-mouse-H3K27me3, anti-mouse-H3K27ac or anti-mouse-H3K9ac; Cosmo Bio) or mouse-IgG (Santa Cruz) as a negative control were used. For ChIP for pCreb1 and Icer, 3 × 10^6 cells and 4 μg of each antibody (anti-rabbit-pCreb1(Ser133); Cell Signaling Technology, anti-rabbit-Crem(X-12); Santa Cruz) or rabbit-IgG (Santa Cruz) as a negative control were used. Immune complexes were captured with 10 μl of M-280 sheep anti-mouse IgG (Life Technologies) or 40 μl of M-280 sheep anti-rabbit IgG (Life Technologies) for 4 h at 4°C. After the beads were washed once with ice-cold RIPA buffer (0.1% SDS, 1% Triton X-100, 50 mM Tris–HCl [pH 8.0], 1 mM EDTA [pH 8.0], 150 mM NaCl, 0.1% sodium deoxycholate), once with ice-cold high-NaCl RIPA buffer (0.1% SDS, 1% Triton X-100, 50 mM Tris–HCl [pH 8.0], 1 mM EDTA [pH 8.0], 300 mM NaCl, 0.1% sodium deoxycholate) and twice with ice-cold TE (10 mM Tris–HCl [pH 8.0], 1 mM EDTA [pH 8.0]), formaldehyde cross-linking was reversed by overnight incubation with 200 μl of ChIP elution buffer (0.5% SDS, 10 mM Tris–HCl [pH 8.0], 5 mM EDTA [pH 8.0], 300 mM NaCl) at 65°C overnight. The immunoprecipitated samples and the same amount of chromatin fragments without IP (input) were treated with proteinase K for 1 h at 55°C, further treated with RNase A (Thermo Scientific) for 30 min at 37°C, and purified by PCI extraction and ethanol precipitation. DNA was resuspended in 20 μl of sterile water and used as a template for quantitative PCR with specific primers (see Supplementary Table S1). The results from three independent experiments were averaged.

Bisulfite sequencing

To determine the DNA methylation profiles of the *Nusap1* promoter regions, genomic DNAs were subjected to the bisulfite reaction using a MethylCode Kit (Life Technologies) according to the manufacturer's instructions. Each bisulfite-treated genome was amplified using AmpliTaq Gold 360 Master Mix (Life Technologies) or LA Taq (TaKaRa) with the primers listed in Supplementary Table S3. Each PCR product was cloned into pGEM T-easy (Promega) and 8 randomly picked clones were sequenced.

Plasmid construction and lentivirus production

Lentiviral vectors pLLX and pLEMPRA (34) were generously provided by Drs Z. Zhou and M. E. Greenberg.

For knockdown experiments, pLLX was used to enable the simultaneous expression of the shRNA and EGFP RNA under the control of U6 and ubiquitin-C promoters, respectively. The sh-RNA oligos were inserted into the HpaI and XhoI sites of pLLX (see Supplementary Table S2).

For rescue experiments, pLEMPRA was used to enable the simultaneous expression of the shRNA and EGFP-IRES-*Nusap1* under the control of U6 and ubiquitin-C promoters, respectively. A FLAG-tagged rat *Nusap1* expression lentiviral vector was constructed by inserting *Nusap1* cDNA between the EcoRI and AscI sites, and inserting the *sh-pancNusap1* sequence between the HpaI and XhoI sites of pLEMPRA (see Supplementary Table S2).

For conditional *pancNusap1*-OE or -KD experiments, we employed the lentivirus-based pSLIK_Neo vector system (Addgene), which allows tight Dox-inducible, RNA polymerase II (RNAPII)-mediated transcription of a gene of interest, and co-expression of a Neomycin selection gene (35). The panc*Nusap1* fragments (−1685 to −323 relative to the TSS of *Nusap1*), isolated by genomic PCR with specific primers (see Supplementary Table S2), were inserted into the SacII and XbaI sites of the entry vector pEN_TmiRc3 (Addgene). The annealed *sh-pancNusap1* oligo (see Supplementary Table S2) was inserted between the HpaI and XhoI sites of pEN_TmiRc3. Recombination of pEN_TmiRc3 and pSLIK_Neo was performed using the LR Clonase Enzyme Mix (Life Technologies) to obtain *pancNusap1*- or *sh-pancNusap1*-expressing vectors according to manufacturer's instructions. We confirmed that Dox-inducible expression of *sh-pancNusap1* successfully caused a reduction of *pancNusap1* expression in the PC12 cell line (Supplementary Figure S1).

HEK 293T cells were used as producers of lentiviruses, and were cultured in high-glucose DMEM (Nacalai Tesque) containing 10% FBS (Biowest) and antibiotics. The expression vector was transfected along with third-generation lentiviral packaging and pseudotyping plasmids (36) using PEI-MAX (COSMO BIO). Ten micrograms of pSLIK, pLLX or pLEMPRA plasmid, 3 μg of the packaging plasmid pCAG-HIVgp and 3 μg of pCMV-VSV-G-RSV-Rev were diluted in 500 μl of Opti-MEM (Gibco) and used for cells in a 10-cm-diameter dish. The medium was replaced after 12 h of transfection. The virus-containing supernatant was collected 48 h later, and the virus was concentrated by centrifugation at 6000 *g* overnight at 4°C, and used for the manipulation of *pancNusap1* or *Nusap1* expression in PC12 cells.

RESULTS

Cell cycle arrest was observed in the irreversible differentiation of NGF/cAMP-differentiated PC12 cells

Clear morphological differences were observed here between Ndiff and NcAdiff cells, as previously documented in the literature (22). NcAdiff cells could be distinguished from Ndiff cells by the thickening of neurites and increase in cell soma size of the former (Figure 1A). To ascertain

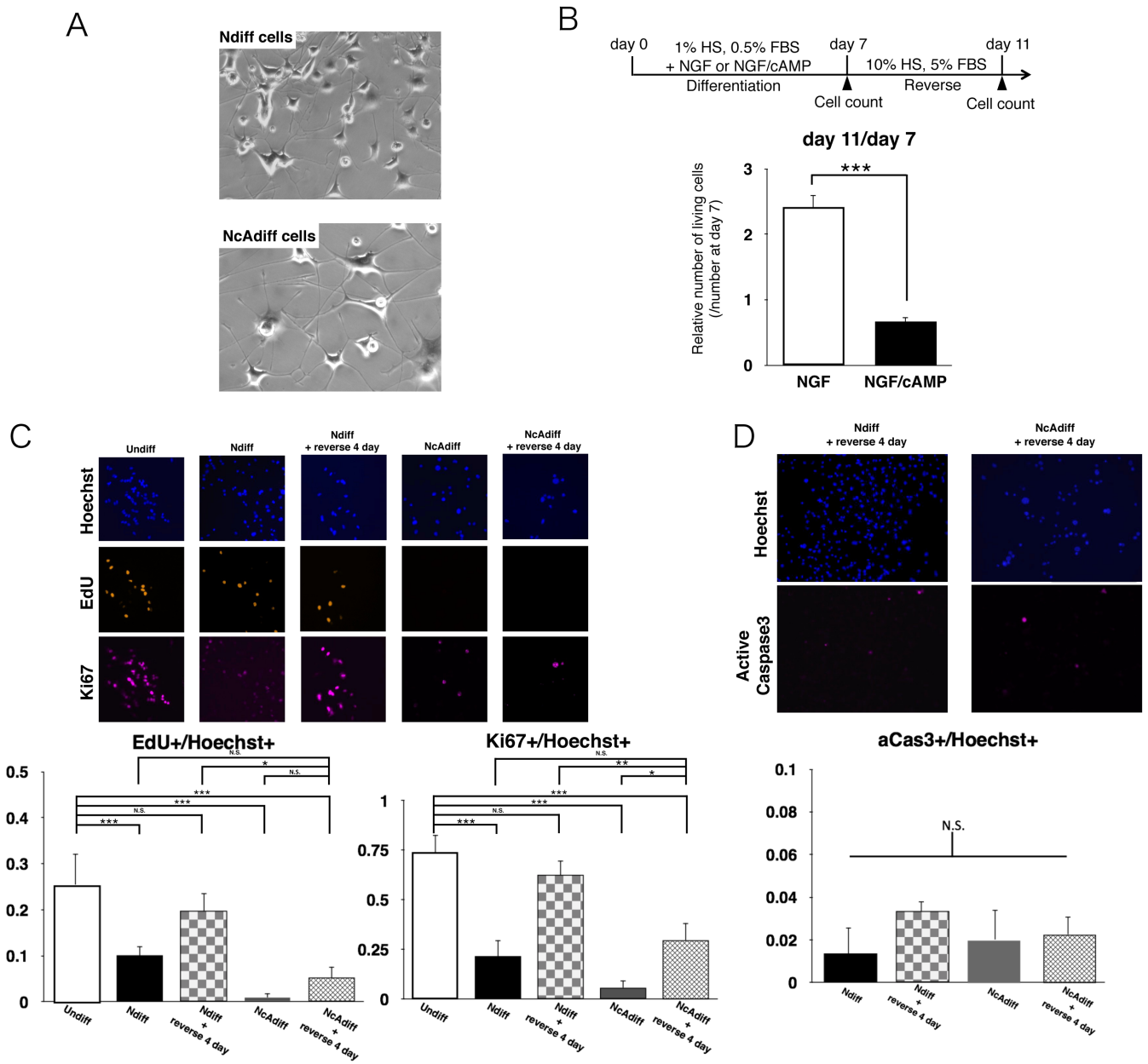

Figure 1. Combination of NGF and cAMP stimulations caused cell cycle arrest in differentiated PC12 cells. (**A**) Morphologies of PC12 cells that grew during 7 days of differentiation in the presence of NGF (upper) or NGF/cAMP (lower). (**B**) Relative number of living cells after removal of NGF or of NGF and cAMP. Upper diagram shows experimental scheme. After 7 days of differentiation of PC12 cells, NGF and cAMP were removed to allow proliferation. Number of living cells was evaluated by counting trypan blue staining-negative cells. Number of cells in each differentiation state at day 7 was set as 1. (**C**) Cell proliferation monitored by EdU incorporation and Ki67 staining in undifferentiated (Undiff), NGF-differentiated (Ndiff) and NGF/cAMP-differentiated (NcAdiff) cells, and in Ndiff and NcAdiff cells after 4 days of incubation in proliferative condition (Ndiff + reverse 4 day, NcAdiff + reverse 4 day, respectively). (**D**) Proportion of apoptotic cells before/after removal of NGF or NGF and cAMP, detected by active Caspase 3 (aCas3) staining. In (**B**–**D**), values are mean ± SD ($n = 3$). Statistical analysis was performed using Student's two-tailed t-tests, or the Tukey-Kramer multiple comparison test. N.S. = not significant. $^{*}P < 0.05$; $^{**}P < 0.01$; $^{***}P < 0.001$.

whether Ndiff and NcAdiff cells showed a difference in the reversibility of their differentiation after removal of these agents, we counted the number of cells after 7 days of differentiation in the presence of NGF or NGF/cAMP followed by 4 days of culture in proliferative conditions without NGF or cAMP (Figure 1B). After the NGF-containing differentiation medium was changed back to the proliferation medium, Ndiff cells resumed proliferation. In contrast, NcAdiff cells did not resume proliferation after such a change. Thus, 7 days of differentiation in the presence of NGF/cAMP induced irreversible differentiation of a fraction of PC12 cells, whereas the differentiation induced NGF alone was reversible. To monitor the cell cycle progression in each cell state, we immunostained incorporated 5-ethynyl-2′-deoxyuridine (EdU) and the proliferation marker Ki67 (Figure 1C). In Ndiff cells, both the EdU+

and the Ki67+ cells decreased by about 40%, compared to undifferentiated (Undiff) PC12 cells. After the NGF-containing differentiation medium was changed back to the proliferation medium, the fractions of both the EdU+ and the Ki67+ cells increased to levels comparable to those of Undiff cells. In contrast, the fractions of both the EdU+ and the Ki67+ cells were very low in NcAdiff cells. Even after the NGF/cAMP-containing differentiation medium was changed back to the proliferation medium, the fractions of both the EdU+ and the Ki67+ cells remained low. Thus, cells continued to proliferate marginally in the NGF-containing differentiation medium, whereas NcAdiff cells almost completely stopped progressing through the cell cycle. To investigate whether apoptosis occurred in each cell state, we immunostained an apoptosis marker, activated Caspase 3 (aCas3; Figure 1D). The fractions of aCas3+ cells were continuously very low, and did not differ markedly among all the samples examined. Taken together, these results showed that cell cycle arrest, but not apoptosis, occurred in the differentiated PC12 cells after the removal of cAMP.

A significant number of M-phase-associated genes were specifically repressed in NcAdiff cells

To identify RNAs whose expression dynamics differed between reversibly and irreversibly differentiated PC12 cells, we performed high-throughput directional sequencing of Undiff, Ndiff and NcAdiff cells using Illumina Hiseq2000. The data contained over 148 million raw reads per sample, with a total of 517 million reads after removing low quality reads (Supplementary Table S4). These reads were mapped to the rat Rn5 reference genome using TopHat2 (see 'Materials and Methods' section). The average percentage of uniquely mapped reads among the valid reads was 81.7% (Supplementary Table S4). Our RNA-seq data showed little 5′-3′ mapping bias for annotated protein-coding genes (Ensembl gene annotation, version 76: Figure 2A) and robust reproducibility among four replicates (Pearson correlation coefficient, $R > 0.98$: Figure 2B). Hierarchical clustering analysis of the sequenced datasets based on the expression levels of protein-coding genes revealed that the expression profiles of protein-coding genes were cell-state-specific and highly reproducible among replicates (Figure 2C). In order to validate the strandedness of our directional RNA-seq data, we mapped the reads to the annotated RefSeq genes and calculated the proportion that mapped on the correct strand, and thereby found that more than 99% of the reads were mapped to the correct strands (Supplementary Table S5). In Ndiff cells, 3346 protein-coding genes showed significantly higher expression levels compared to those in NcAdiff cells (q-value < 0.05). Gene Ontology analysis of these Ndiff PC12-specific protein-coding genes revealed a strong enrichment in the Gene Ontology biological process terms associated with cell cycle, especially terms related to G2/M-phase progression (e.g., mitotic cell cycle, M phase and mitotic M phase: Figure 2D), which is consistent with our finding that cell cycle arrest was observed much more frequently in NcAdiff cells than in Ndiff cells (Figure 1C).

pancRNA and mRNA pairs were possible downstream targets of cAMP signaling pathway

Impey *et al*. reported that more than half of total pCreb1-binding sites are located adjacent to genes, and in particular, pCreb1-binding regions are significantly enriched in bidirectional promoters that produce annotated transcripts in both directions (annotated bidirectional promoters or aBiPs) (15). Recent studies have revealed that antisense noncoding transcripts are derived from upstream of many protein-coding genes in mammals (7,11,37). We therefore hypothesized that not only aBiPs, but also protein-coding gene promoters that simultaneously produce pancRNAs (pancRNA-associated bidirectional promoters or pBiPs) were potential targets of transcriptional regulation by a CRE-mediated mechanism.

To test our hypothesis, first, we adjusted the annotated TSSs of genes according to our directional RNA-seq data in order to improve the accuracy of prediction of pBiPs (see 'Materials and Methods' section). Next, because MACS2 showed more sensitivity and accuracy for detection of lncRNA than transcript models reconstructed using *ab initio* transcript assembly tools (e.g. Cufflinks and Trinity; Supplementary Figure S2), we identified the read-enriched regions using MACS2 software after parameter setting, and classified these regions according to their positions relative to those of annotated transcripts. A total of 51 939 regions were classified as regions of non-annotated transcripts. Of these, 2758 regions were classified as regions of candidate-pancRNAs, which were overlapped with the 1-kb region upstream of the TSS of an annotated protein-coding gene in an antisense direction. The average length of the candidate-pancRNAs was 1928 bp, and the average distance between the 5′ ends of candidate-pancRNAs and that of its partnered gene was 167 bp (Supplementary Figure S3). As expected, based on coding potential estimation using the CPC algorithm (27), 92.5% of the non-annotated transcripts and 96.9% of candidate-pancRNAs exhibited negative coding potential scores, suggesting that most of these regions can be regarded as templates of pancRNAs (Figure 3A). We regarded the annotated protein-coding gene promoters producing pancRNAs as pBiPs. As a result, we identified 3235 bidirectional promoters in PC12 cells. Of these, 948 genes derived from 474 out of 477 aBiPs, 2718 pancRNAs and their paired genes derived from 2718 out of 2758 pBiPs were transcribed in Undiff, Ndiff or NcAdiff cells.

Then, we investigated the frequency of CRE occurrence in aBiPs and pBiPs. There were one or more CRE sequences in 27.6% of all protein-coding gene promoters (−1000 to +1000 bp from the TSS) and in 36.1% of aBiPs and 32.3% of pBiPs. Thus, in agreement with our hypothesis, CRE sequences were highly enriched not only in aBiPs, but also in pBiPs compared to all protein-coding gene promoters (Figure 3B). To further validate our hypothesis, we analyzed a publicly available pCreb1 ChIP-seq dataset of PC12 cells immediately after cAMP signal activation by forskolin (15). Investigation of the frequency of overlap of pCreb1-binding at protein-coding gene promoters showed that pCreb interacted with 59% of aBiPs, 45% of pBiPs and 23% of all protein-coding gene promoters. Similarly, we analyzed a publicly available Creb1 ChIP-seq dataset of E16.5 mouse

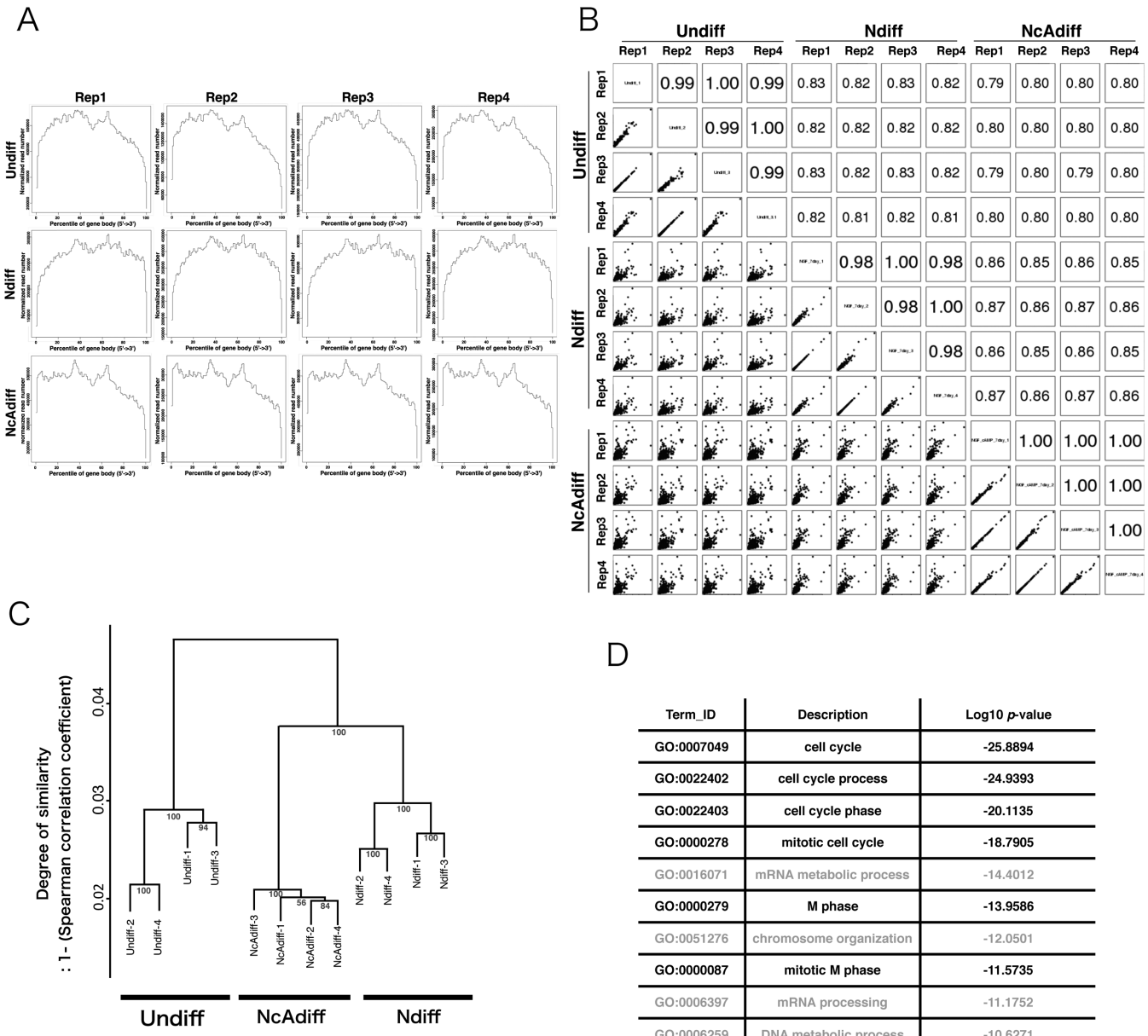

D

Term_ID	Description	Log10 *p*-value
GO:0007049	cell cycle	-25.8894
GO:0022402	cell cycle process	-24.9393
GO:0022403	cell cycle phase	-20.1135
GO:0000278	mitotic cell cycle	-18.7905
GO:0016071	mRNA metabolic process	-14.4012
GO:0000279	M phase	-13.9586
GO:0051276	chromosome organization	-12.0501
GO:0000087	mitotic M phase	-11.5735
GO:0006397	mRNA processing	-11.1752
GO:0006259	DNA metabolic process	-10.6271

Figure 2. A significant number of M-phase associated genes were not stringently repressed in Ndiff cells. (**A**) Density plots of directional RNA-seq reads mapped to the RefSeq genes to evaluate 5′-3′ potential mapping bias across genes. Each sample category consisted of four replicates (Rep1–4). (**B**) Scatter plots of gene expression levels and Pearson correlation coefficients among all sequenced samples. The expression levels of genes were calculated based on the number of reads mapped to each Ensembl protein-coding gene normalized by iDEGES/edgeR methods. (**C**) Hierarchical clustering of sequence data sets based on the expression levels of Ensembl protein-coding genes. The distance between samples was determined by clustering using group average methods and linkage criteria based on Spearman's rank coefficient of correlation. The numbers in tree diagrams are approximately unbiased *P*-values. (**D**) The top 10 most significantly enriched GO terms for 3346 Ndiff-specific protein-coding genes. The *P*-value is the Benjamini–Hochberg corrected *P*-value.

cortical neurons that had been maintained *in vitro* for 7 days (32). Creb1 binding signals were significantly enriched not only in aBiPs, but also in pBiPs (Supplementary Figure S4). These results supported our hypothesis that not only aBiPs but also pBiPs were preferred downstream targets of cAMP signaling during the irreversible differentiation of PC12 cells.

Next, because the expression of pancRNA and the corresponding annotated protein-coding gene are positively correlated in both mouse and human brain (11,38), we investigated whether the expression dynamics of pancRNA–mRNA pairs were also positively correlated during the differentiation of PC12 cells. First, we calculated the correlation coefficient of the expression level of each RNA pair during PC12 differentiation, and then classified them into three groups. The first group was composed of antisense lncRNAs that overlapped with the 1-kb region upstream from the 5′ ends of mRNAs and the partner mRNAs (pancRNA–mRNA pairs). The second group was composed of antisense lncRNAs that overlapped with the 1-kb

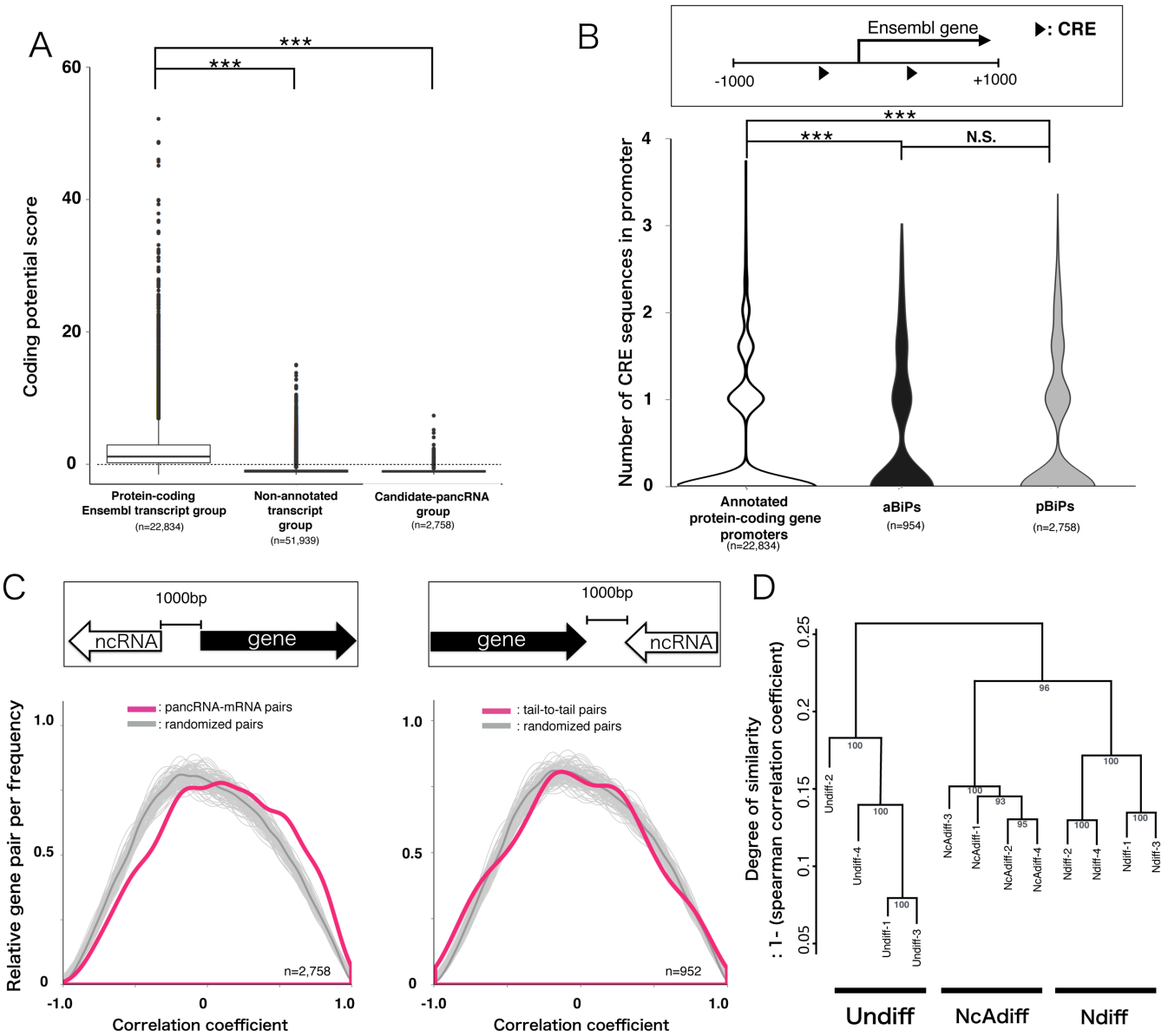

Figure 3. The bidirectional promoters driving pancRNAs can be novel targets of cAMP signaling. (**A**) Distribution of coding potential scores for annotated protein-coding Ensembl transcripts, non-annotated transcripts and candidate-pancRNAs using the CPC algorithm. Negative scores indicate low coding potential. (**B**) Distribution of numbers of CREs located in the promoters (−1000 to +1000 from TSS) of all protein-coding genes, genes derived from aBiPs and pBiPs. (**C**) Distribution of Pearson correlation coefficients calculated based on the expression of protein-coding genes and nearest novel lncRNAs (magenta curve). The dark gray lines show the average correlation coefficient distribution based on 200 permutations of 2000 randomly selected pairs of lncRNAs and protein-coding gene. The pale gray lines represent 200 simulation results. Significance was calculated with the Mann–Whitney U test (left: $P < 2.2e\text{-}16$; right: $P = 0.59$). (**D**) Hierarchical clustering of sequence data sets based on pancRNA expression levels. The distance between samples was determined by clustering using group average methods and linkage criteria based on Spearman's rank coefficient of correlation. The numbers in tree diagrams are approximately unbiased *P*-values. Statistical analysis was performed using the Tukey-Kramer multiple comparison test in (A and B). N.S. = not significant. $***P < 0.001$.

region downstream from the 3′ ends of mRNAs and the partner mRNAs (tail-to-tail pairs). The third group was composed of randomly selected RNA transcripts (randomized pairs). We found that the distribution of the correlation coefficients of the pancRNA–mRNA pairs was significantly different from that of the tail-to-tail pairs (Bonferroni-corrected Mann–Whitney U test, $P < 2.1e\text{-}9$) and that of randomized pairs ($P < 2e\text{-}16$; Figure 3C left). However, no significant difference was observed between the distribution of the correlation coefficients of the tail-to-tail pairs and that of randomized pairs ($P = 0.99$; Figure 3C right). These statistical analyses highlighted the positive correlation of pancRNA–mRNA expression during PC12 differentiation. The hierarchical clustering analysis of sequenced datasets based on candidate-pancRNA expression levels revealed that the expression profiles of candidate-pancRNAs were cell-state-specific and highly reproducible among replicates (Figure 3D). These genome-wide analyses supported

the notion that pancRNAs are physically associated with cAMP targets for the partner gene activation.

After irreversible differentiation, both *Nusap1* and *pancNusap1* expression levels, and the histone acetylation level of the *Nusap1* promoter, were dramatically decreased

Among candidate-pancRNAs, we then focused on a pancRNA from the promoter of a spindle-formation-associated gene *Nusap1* in an attempt to elucidate possible functions of this pancRNA. This pancRNA and its paired annotated protein-coding gene pair exhibited the highest Pearson correlation coefficient among all pancRNA–mRNA pairs during PC12 differentiation ($P = 0.995$: Figure 4A). However, the RNA-seq data showed that there was no coordination of the expression changes of any *Nusap1*-neighboring genes with that of *Nusap1* and its pancRNA (Supplementary Figure S5). We named this pancRNA *pancNusap1*. Its expression as estimated by RNA-seq analysis was lowest in NcAdiff cells among all of the cell samples examined. TGACG, one of the previously identified non-canonical CREs (15), was symmetrically located at −12 and −380 bp relative to the TSS of *Nusap1* (Figure 4C, black arrowheads). Similarly, CGCCA (33) was located at +31 and −230 bp relative to the TSS of *Nusap1* (Figure 4C, gray arrowheads, Supplementary Figure S6). These non-canonical CREs also appeared near the *Nusap1* TSS in the mouse and human genomes (Supplementary Figure S6). We then examined the expression patterns of *pancNusap1* and *Nusap1* in each differentiation state of PC12 cells. As shown in Figure 4B, the expression dynamics of *pancNusap1* as determined by RT-qPCR seemed to be positively correlated with those of *Nusap1*. We confirmed that the expression levels of both *Nusap1* and *pancNusap1* were significantly lower in NcAdiff cells than in Ndiff cells. Interestingly, these lower levels of *pancNusap1* and *Nusap1* expression seemed to continue after NcAdiff cells were put back under proliferative conditions. That is, after the NGF-containing differentiation medium was changed back to the proliferation medium, the expression levels of both *Nusap1* and *pancNusap1* in Ndiff cells recovered to a level similar to that in Undiff cells, whereas the expression levels of both *Nusap1* and *pancNusap1* in NcAdiff cells failed to fully recover after 4 days in proliferative condition.

Since we reported that the expression changes of pancRNAs caused a regional alteration in the epigenetic states in the pBiPs (8), next we examined the epigenetic state of the *Nusap1* promoter by means of bisulfite sequencing and ChIP-qPCR assay. The DNA methylation states were not changed upon differentiation in PC12 cells (Figure 4C). However, the levels of active histone modifications, such as histone H3 lysine 9 acetylation (H3K9ac) and lysine 27 acetylation (H3K27ac), were lower in NcAdiff cells than in Undiff and Ndiff cells (Figure 4D and E). The levels of signals of H3K9ac and H3K27ac on the *Nusap1* promoter in NcAdiff cells remained very low after the differentiation medium was changed back to the proliferation medium (Figure 4E). These kinetics of the histone acetylation levels were concordant with the *pancNusap1* expression pattern, raising the possibility that *pancNusap1* is required for local open chromatin formation, and cessation of the expression of *pancNusap1* causes histone deacetylation at the *Nusap1* promoter. Histone methylation levels, such as the active histone modification histone H3 lysine 4 tri-methylation (H3K4me3), and the repressive histone modifications histone H3 lysine 9 tri-methylation (H3K9me3) and lysine 27 tri-methylation (H3K27me3), were not different between Ndiff and NcAdiff cells (Figure 4D). Taken together, these results indicate that *pancNusap1* expression is associated with local histone acetylation specifically in a cAMP-minus condition.

Knockdown of *pancNusap1* induced a closed chromatin structure in the *Nusap1* promoter, resulting in cell cycle arrest

To test the hypothesis that the regulation of *pancNusap1* is critical for irreversible differentiation, first we examined the effects of *pancNusap1* KD on the expression levels of *Nusap1* in the cells under reversible differentiation condition (see 'Materials and Methods' section). Both of the tested shRNAs for *pancNusap1* downregulated the expressions of not only *pancNusap1* but also *Nusap1* in Ndiff cells (Figure 5A and Supplementary Figure S7). We confirmed that neither of the shRNAs for *pancNusap1* showed off-target effects (Supplementary Figure S8). Next, we investigated the effect of *pancNusap1*-KD on the histone acetylation profile in the *Nusap1* promoter. ChIP-qPCR analysis revealed that *pancNusap1*-KD significantly decreased the signals of both H3K9ac and H3K27ac in the *Nusap1* promoter without affecting the signal levels in the *Gapdh* promoter (Figure 5B and Supplementary Figure S9). Then we examined whether *pancNusap1*-KD affected the proliferation of Ndiff cells after they were returned to the proliferation medium. Counting the living cells revealed that *pancNusap1*-KD inhibited the proliferation of Ndiff cells after the NGF-containing differentiation medium was changed to the proliferation medium (Figure 5C). Moreover, consistent with our hypothesis, immunostaining showed that *pancNusap1*-KD decreased both the EdU+ and the Ki67+ cells even after the NGF-containing differentiation medium was changed back to the proliferation medium (Figure 5D). Thus, repression of *pancNusap1* mimics the epigenetic features of irreversibly differentiated PC12 cells.

Overexpression of *pancNusap1* induced cell cycle progression with an open chromatin formation in the *Nusap1* promoter

To further test our hypothesis that regulation of *pancNusap1* is critical for irreversible differentiation, we examined the effects of *pancNusap1* OE on the expression levels of *Nusap1* in NcAdiff cells. Since *pancNusap1* contained regions highly homologous with mouse *Oip5* (Figure 6A), it seemed possible that this pancRNA might need to be translated in order for it to function. However, when we used a genomic region lacking the predicted translation initiation site (*pancNusap1ΔTIS*), we still found upregulation of *Nusap1* (Figure 6B). Because we discovered previously that several pancRNAs function in a strand-specific manner (8), we also prepared PC12 cells in which the strand opposite *pancNusap1* (*sense_pancNusap1ΔTIS*) was exogenously expressed (Figure 6A), and found that

A

Ensembl gene ID : gene name	Correlation coefficient	Normalized read counts of pancRNA in Ndiff cells	Normalized read counts of pancRNA in NcAdiff cells	Log_2(Ndiff/NcAdiff)
ENSRNOG00000004921:Nusap1	0.996	1142.340	373.754	1.612
ENSRNOG00000013920:Arhgap26	0.979	1300.450	2337.300	-0.846
ENSRNOG00000012347:Gata2	0.970	20971.300	8365.470	1.326
ENSRNOG00000010435:Nupl2	0.970	277.657	176.517	0.653
ENSRNOG00000021839:RGD1563556	0.967	615.537	253.741	1.278
ENSRNOG00000016534:Fam171a1	0.962	3277.990	8169.870	-1.318
ENSRNOG00000027249:Fancl	0.956	85.277	35.207	1.276
ENSRNOG00000020274:Taf5	0.951	365.662	212.179	0.785
ENSRNOG00000049849:Fam199x	0.941	464.205	309.653	0.584
ENSRNOG00000005332:Csdc2	0.940	1145.180	2045.300	-0.837

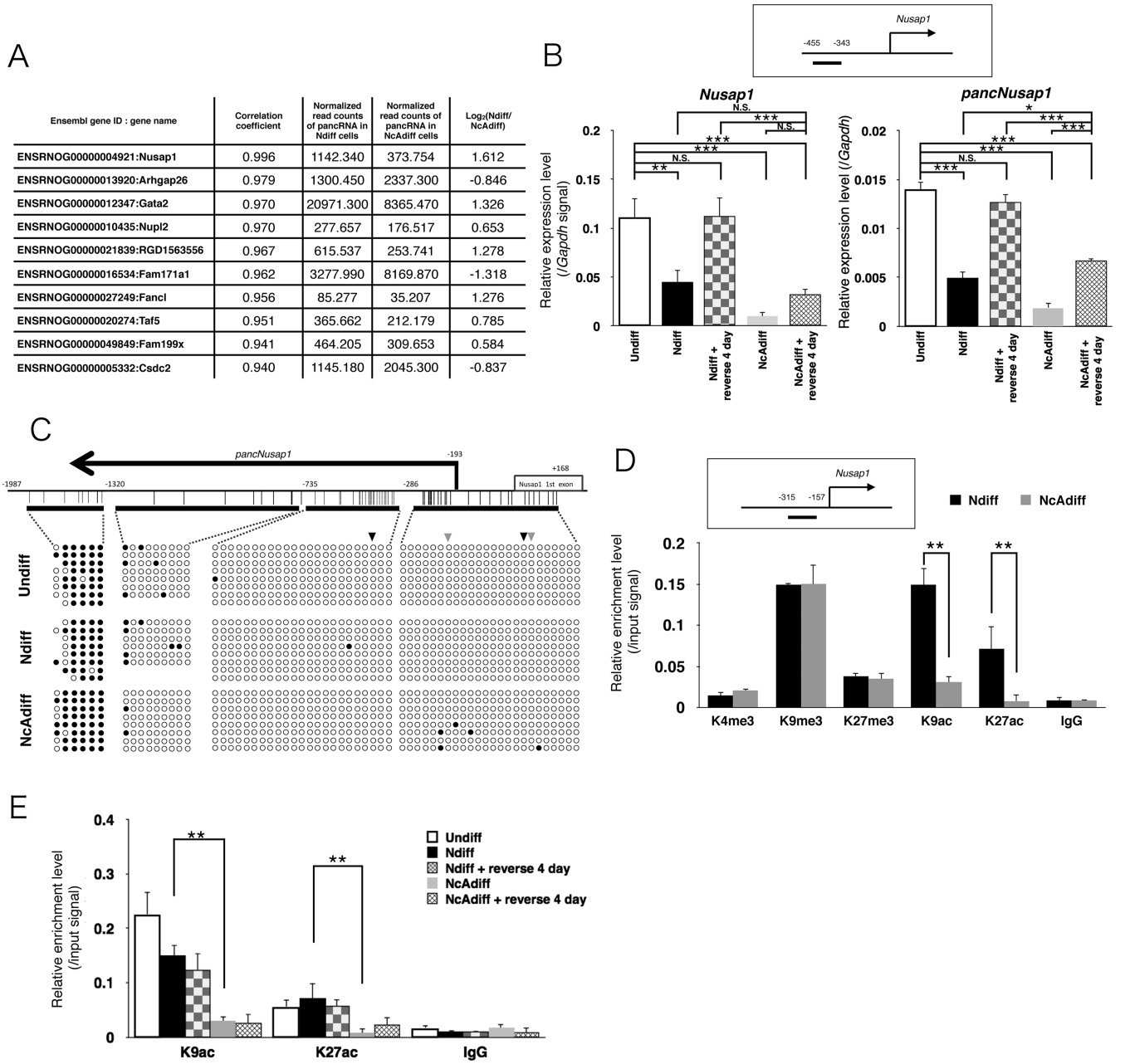

Figure 4. Both *Nusap1* and *pancNusap1* were epigenetically repressed in NcAdiff cells. (**A**) List of the top 10 candidate-pancRNA/mRNA pairs showing highest correlation of expression during PC12 differentiation. The expression levels of pancRNAs normalized with the iDEGES/edgeR method are also shown. (**B**) RT-qPCR analysis of *pancNusap1* and *Nusap1* in Undiff, Ndiff and NcAdiff cells, before and after NGF and cAMP factor deprivation. Upper diagram shows the location of the primer used for RT-qPCR of *pancNusap1*. *Gapdh* was used as a control. (**C**) DNA methylation levels of the *Nusap1* promoter region in Undiff, Ndiff and NcAdiff cells. Upper diagram shows the genomic structure of the rat *Nusap1* promoter. Thick horizontal lines indicate the regions analyzed by bisulfite sequencing. Vertical lines mark the location of CpG dinucleotides. Primer positions are numbered relative to TSS of the *Nusap1* gene. Filled and empty circles indicate methylated and unmethylated cytosines, respectively. Black and gray arrowheads indicate locations of the previously identified non-canonical CRE, TGACG and CGCCA, respectively. (**D** and **E**) Histone modification status of the *Nusap1* promoter in each differentiation state of PC12 cells. Upper diagram shows the location of the primers used in the ChIP assay. Status of histone H3 lysine 4 tri-methylation (H3K4me3), lysine 9 tri-methylation (H3K9me3), lysine 27 tri-methylation (H3K27me3), histone H3 lysine 9 acetylation (H3K9ac) and lysine 27 acetylation (H3K27ac) was evaluated. Normal mouse IgG (IgG) was used as a negative control. The same amount of chromatin fragments as used for each immunoprecipitation was also subjected to PCR without IP as a positive control (Input). In (B), (D) and (E), values are mean ± SD ($n = 3$). Statistical analysis was performed using Student's two-tailed *t*-tests, or the Tukey-Kramer multiple comparison test. N.S. = not significant. $^{**}P < 0.01$; $^{***}P < 0.001$.

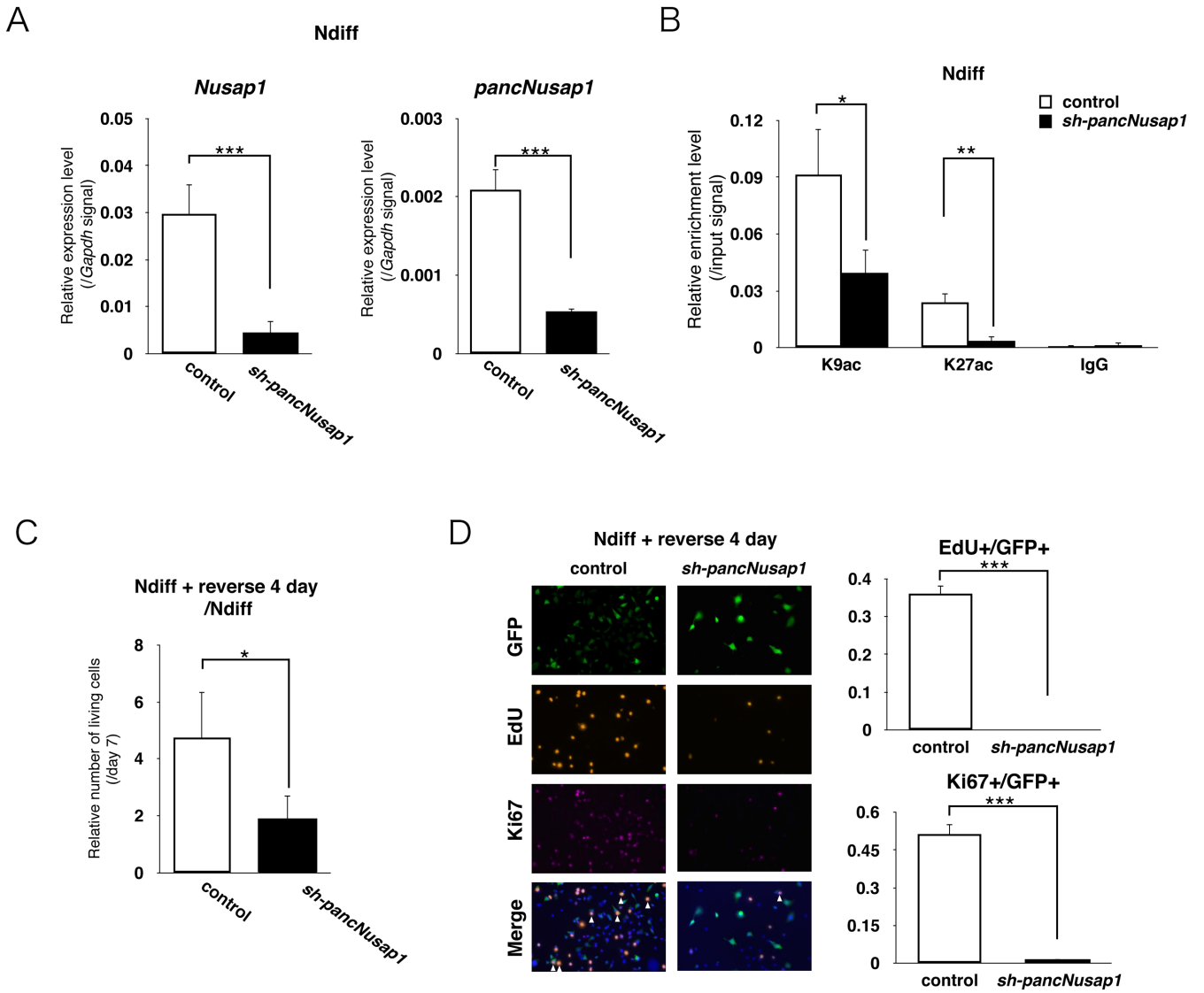

Figure 5. Knockdown (KD) of *pancNusap1* mimicked irreversible differentiation of PC12 cells induced by cAMP (**A**) The effect of *pancNusap1* KD on the expression level of *Nusap1* in Ndiff cells. *Gapdh* was used as a control. Empty vector-introduced PC12 cells were used as a negative control. (**B**) Histone modification status of the *Nusap1* promoter in *pancNusap1*-KD PC12 cells under reversible differentiation condition. The expression of *sh-pancNusap1* was induced by Dox at day 5. Empty vector-infected PC12 cells were used as a control. (**C**) The effects of *pancNusap1* KD on cell proliferation in Ndiff cells. The numbers of living cells were counted. (**D**) Proportion of the EdU+ and the Ki67+ cells in *pancNusap1*-KD PC12 cells after NGF deprivation. After 7 days of differentiation, NGF was removed to allow proliferation. White arrowheads indicate locations of proliferating infected cells (triple-positive for Ki67, EdU and GFP). In (A–C), viral vectors were introduced at day 3. In (A–D), values are mean ± SD ($n = 3$). Statistical analysis was performed using Student's two-tailed *t*-tests, or the Tukey-Kramer multiple comparison test. N.S. = not significant. $*P < 0.05$; $**P < 0.01$; $***P < 0.001$.

the introduction of *sense_pancNusap1ΔTIS* could not up-regulate the expression of *Nusap1* (Figure 6B). This indicates that the direction of transcription of this pancRNA was important for its function as a local gene activator. We also investigated the effect of *pancNusap1ΔTIS*-OE and *sense_pancNusap1ΔTIS*-OE on the histone acetylation profile of the *Nusap1* promoter in NcAdiff cells, and found that *pancNusap1ΔTIS*-OE, but not *sense_pancNusap1ΔTIS*-OE, increased the signals of both H3K9ac and H3K27ac at the *Nusap1* promoter in parallel with *Nusap1* upregulation (Figure 6C). Then, to investigate the effects of *pancNusap1*-OE on the phenotypic irreversibility of PC12 cells, we immunostained PC12 cells with antibody against Ki67 and counted the number of living cells before/after the NGF/cAMP-containing medium was changed back to the proliferation medium, and found that the number of cells was increased by *pancNusap1ΔTIS*-OE, but not by *sense_pancNusap1ΔTIS*-OE (Figure 6A and D). Immunostaining revealed an increase of the Ki67+ cells after *pancNusap1ΔTIS*-OE (Figure 6E), indicating that re-proliferation was enhanced by *pancNusap1ΔTIS*-OE. These data showed that *pancNusap1ΔTIS*-OE expression could induce morphological and epigenetic features characteristic of the reversibly differentiated state of PC12 cells in irreversibly differentiated cells.

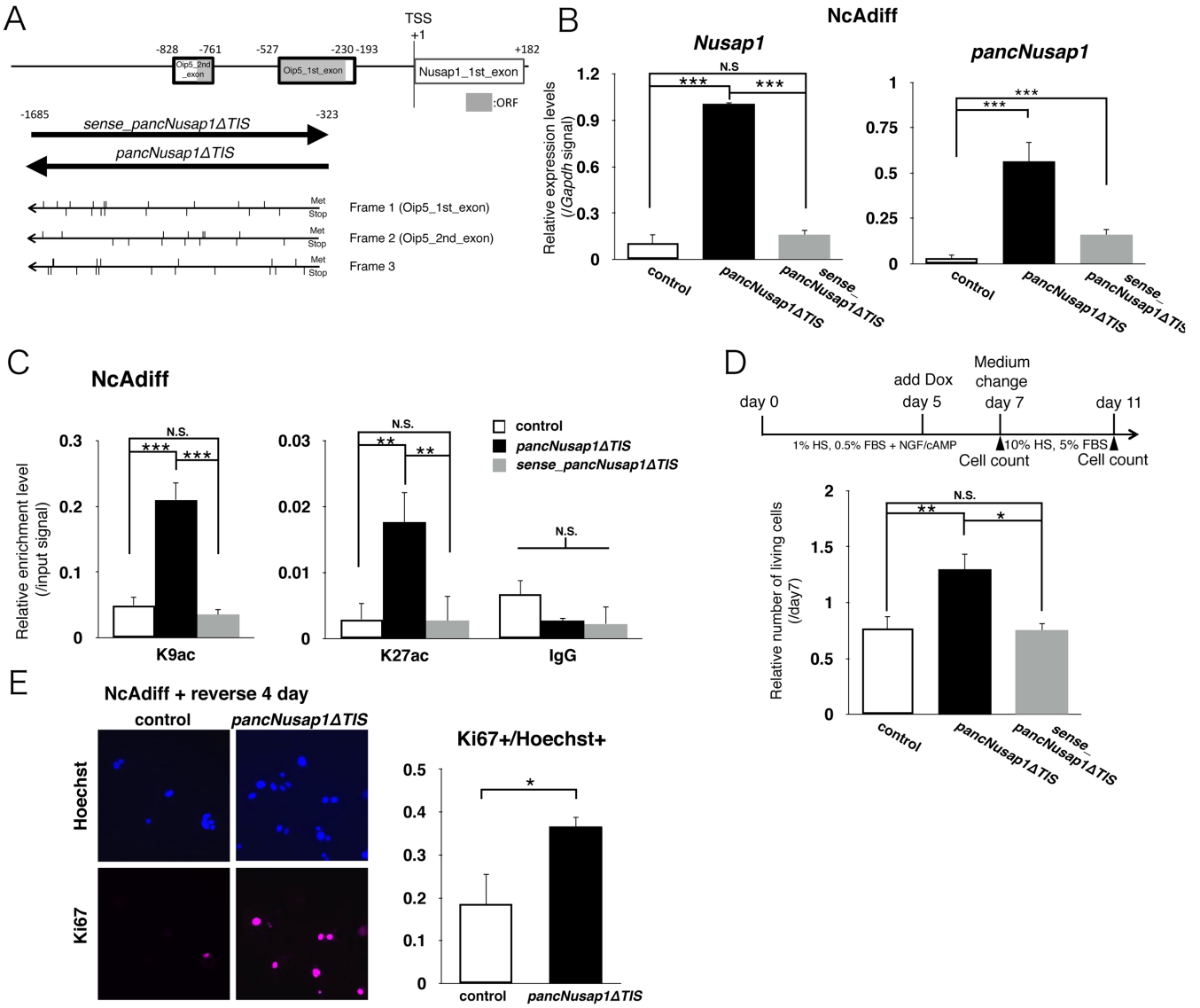

Figure 6. *pancNusap1* overexpression (OE) caused cells subjected to the irreversibly differentiation condition to have the morphological and epigenetic characters of reversibly differentiated cells. (**A**) Genomic structure of the rat *Nusap1* promoter. Bold-lined boxes show the region homologous to mouse *Oip5*. Gray boxes indicate predicted locations composing the *Oip5* open reading frame (ORF). Lower thick arrows indicate the region and transcribed strands used for OE-experiments of ncRNA. Upper and lower vertical lines show the positions of methionines (Met) or stop codons (Stop), respectively, in each translational frame. (**B**) The effect of Dox-induced sense or antisense *pancNusap1* OE on the *Nusap1* expression level in NcAdiff cells. *Gapdh* was used as a control. Empty vector-introduced PC12 cells were used as a negative control. (**C**) Histone modification status of the *Nusap1* promoter in *pancNusap1*-overexpressing PC12 cells under irreversible differentiation condition. (**D**) The effect of Dox-induced sense or antisense *pancNusap1* OE on cell proliferation in NcAdiff cells. Upper diagram shows experimental scheme. Number of living cells was counted. After 7 days of differentiation of PC12 cells, NGF/cAMP were removed to allow proliferation. (**E**) Proportion of Ki67+ cells in antisense *pancNusap1*-overexpressing PC12 cells after NGF/cAMP deprivation. In (B–E), values are mean ± SD ($n = 3$). Statistical analysis was performed using Student's two-tailed *t*-tests or the Tukey-Kramer multiple comparison test. N.S. = not significant. $*P < 0.05$; $**P < 0.01$; $***P < 0.001$.

Overexpression of *Nusap1* rescued *pancNusap1*-KD-induced cell cycle arrest

To test the epigenetic effects of *pancNusap1*-KD and -OE in a single gene expression setting, we performed rescue experiments of *pancNusap1*-KD cells with *Nusap1*-OE, and monitored the proliferation of Undiff or Ndiff cells after introduction of *sh-pancNusap1* and *Nusap1*. In Undiff cells, the reductions of both the EdU+ and the Ki67+ cells by *pancNusap1*-KD were rescued by the simultaneous introduction of *Nusap1*-OE (Figure 7A and Supplementary Figure S10). Counting the number of living cells after 4 days of culture in re-proliferative condition further confirmed that, after the NGF-containing differentiation medium was changed back to the proliferation medium, the reduction of the number of cells by *pancNusap1*-KD was successfully rescued by simultaneous *Nusap1*-OE expression (Figure 7B). These results clearly indicate that *pancNusap1* acts to up-regulate the transcription of *Nusap1*.

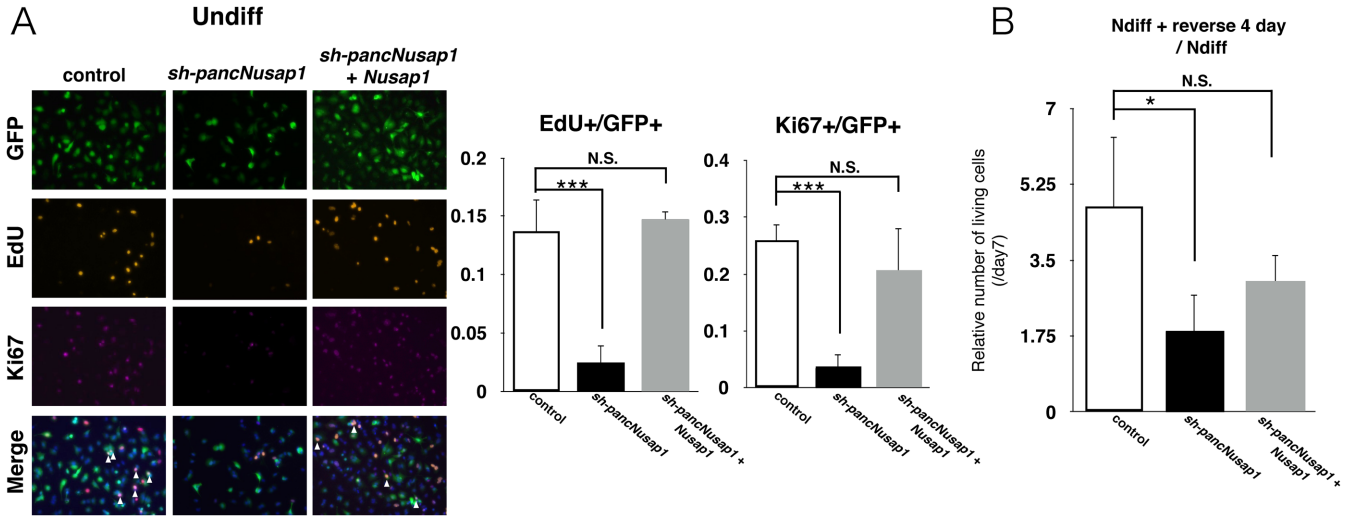

Figure 7. *pancNusap1* regulates irreversibility of PC12 differentiation through transcriptional regulation of *Nusap1*. (**A**) Proportion of the EdU+ and the Ki67+ cells in *pancNusap1*-KD and *Nusap1*-OE Undiff cells. White arrowheads indicate locations of the proliferating infected cells (triple-positive for Ki67, EdU and GFP). (**B**) The effect of *Nusap1*-OE on cell proliferation in the *pancNusap1*-KD cells. Number of living cells was counted. In (A and B), values are mean ± SD ($n = 3$). Statistical analysis was performed using the Tukey-Kramer multiple comparison test. N.S. = not significant. *$P < 0.05$; ***$P < 0.001$.

The activities of pBiPs, including that for the *pancNusap1-Nusap1* pair, were regulated by cAMP signaling

By using the publicly available pCreb1 ChIP-seq dataset of PC12 cells (15), we found that pCreb1 interacted with the *Nusap1* promoter immediately after cAMP signal activation by forskolin. However, because *pancNusap1* and *Nusap1* were silenced in response to cAMP stimulation in NcAdiff cells (Figure 4B), we tried to experimentally confirm the pCreb1-binding at the *Nusap1* promoter and to identify the factors that shut down cAMP-dependent activation of the *pancNusap1–Nusap1* pair as well. Some reports showed that transcription of a dominant-negative form of *Crem*, *Icer* (Supplementary Figure S11A), is activated by binding of pCreb1 after cAMP treatment in PC12 cells (19,39), and therefore we investigated the transcriptional dynamics of *Creb1*, *Crem* and *Icer* using our RNA-seq data. Consistent with previous reports, we found that transcription of *Icer* was dramatically activated in NcAdiff cells (Supplementary Figure S11B). We confirmed these results by RT-qPCR (Supplementary Figure S11C). Next, we performed time-course ChIP experiments to examine the binding of pCreb1 and Icer to the *Nusap1* promoter after NGF/cAMP treatment (Figure 8A). We found that pCreb1-binding was upregulated at 3 h and then diminished by 72 h after the NGF/cAMP treatment. In contrast, Icer-binding was upregulated at 3 h but then partially maintained until 72 h after the NGF/cAMP treatment. These ChIP-qPCR data agree well with the RT-qPCR data, in which both *Nusap1* and *pancNusap1* transcripts were reduced to the basal levels by 72 h (Figure 8B). To further validate the differential roles of pCreb1 and Icer in the transcriptional regulation of the *Nusap1* promoter during PC12 differentiation, we examined the effects of *Icer* and *Creb1* KD on the expression levels of *Nusap1* and *pancNusap1*. As expected, our shRNAs specifically targeted *Icer* or *Creb1,* resulting in their significant downregulation (Figure 8C and Supplementary Figure S12). KD of *Icer* upregulated the expression levels of both *pancNusap1* and *Nusap1* in NcAdiff cells (Figure 8D). In contrast, KD of *Creb1* did not affect the expression levels of either *Nusap1* or *pancNusap1* in NcAdiff cells (Figure 8D). Taking these results all together, we concluded that cAMP signaling represses *pancNusap1* and *Nusap1* through Icer, leading ultimately to the reduction of *Nusap1* expression via *pancNusap1* downregulation.

Finally, to investigate whether pBiPs other than the *Nusap1* promoter were transcriptionally regulated by downstream transcription factors of the cAMP signaling pathway, we examined the effects of *Icer* and *Creb1* KD on the expression levels of two genes listed next to *Nusap1*: *Arhgap26* and *Gata2* (Figure 4A, Supplementary Table S6). We found that in NcAdiff cells, KD of *Icer* significantly upregulated the expression level of *Arhgap26,* and KD of *Creb1* significantly downregulated the expression level of *Gata2* (Figure S13). These results indicated that *Icer* and *Creb1* were involved in the transcriptional regulation of *Arhgap26* and *Gata2,* respectively, and supported our notion that pBiPs are preferred targets of downstream transcription factors of cAMP signaling during the irreversible differentiation of PC12 cells.

DISCUSSION

In this study, we utilized PC12 cells as a model for understanding the bidirectional promoter-mediated mechanism underlying cAMP-triggered irreversible differentiation. Genome-wide analysis of our directional RNA-seq dataset and the publicly available pCreb1 ChIP-seq dataset of PC12 cells (15) revealed that bidirectional promoters for the expression of pancRNA–mRNA pairs are preferred downstream targets of cAMP signaling during the irreversible differentiation of PC12 cells. In irreversibly differentiated PC12 cells, the activities of representative bidirectional promoters for the expression of pancRNA–mRNA

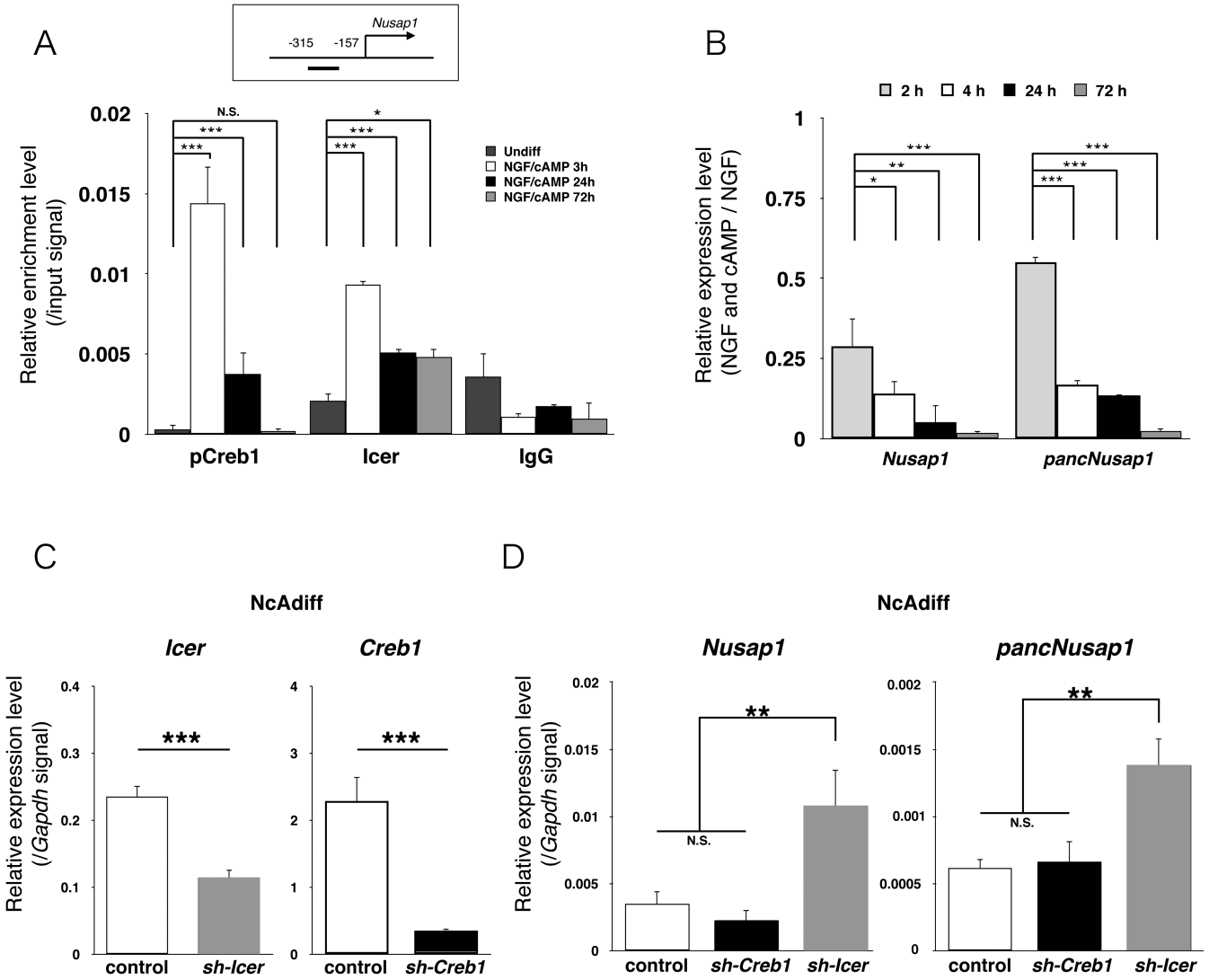

Figure 8. The transcriptional activity of *pancNusap1-Nusap1* pair was regulated by Icer after cAMP stimulation. (**A**) pCreb1- and Icer-binding status at the *Nusap1* promoter after 3, 24 and 72 h of NGF/cAMP treatment. Normal rabbit IgG (IgG) was used as a negative control. (**B**) The expression dynamics of *pancNusap1* and *Nusap1* after 2, 4, 24 and 72 h of NGF and/or cAMP treatment. (**C** and **D**) The effects of *sh-Icer* and *sh-Creb* OEs on the expression levels of their target genes (C) and the *pancNusap1-Nusap1* pair (D) in NcAdiff cells. Viral vectors were introduced at day 3. In (A–D), values are mean ± SD ($n = 3$). Statistical analysis was performed using the Tukey-Kramer multiple comparison test. N.S. = not significant. $^{*}P < 0.05$; $^{**}P < 0.01$; $^{***}P < 0.001$.

pairs were regulated by transcription factors in the cAMP-dependent pathway (Figure 8 and Supplementary Figure S13). To examine whether such transcriptional regulation of pancRNA–mRNA pairs contributes to the cAMP-triggered irreversible differentiation, we focused on *pancNusap1* and *Nusap1,* the pancRNA–mRNA pair showing the highest Pearson correlation coefficients of the expression during PC12 differentiation. KD and OE experiments showed that *pancNusap1* positively regulated the *Nusap1* expression in a sequence-specific manner, which was accompanied by acetylation of histone H3 lysine 9 and 27 at the promoter. Both the *pancNusap1* and the *Nusap1* expression levels and the histone acetylation level of the *Nusap1* promoter decreased concomitantly, most likely as part of the regulation responsible for irreversible differentiation, as shown by our finding that the epigenetic silencing of *Nusap1* via KD of *pancNusap1* recapitulated the cAMP effect on cell cycle arrest during the process of irreversible differentiation of PC12 cells.

Downstream transcription factors of cAMP signaling regulate the expression of hundreds of gene activation-associated ncRNAs derived from bidirectional promoters

A previous ChIP-seq study showed that a quarter of pCreb1-target genes are derived from aBiPs, suggesting that such head-to-head promoter structures may provide adaptive advantages for cAMP functioning in cells (15). In this study, we showed that annotated protein-coding genes were expressed from 474 aBiPs, and from 2718 pBiPs, in rat PC12 cells. Genome-wide analysis, supported by representative experimental tests, revealed that not only aBiPs but

also pBiPs were enriched for CRE consensus sequences, and were preferential targets for regulation by the transcription factors in the cAMP-dependent pathway (Figures 3B and 8 and Supplementary Figure S13). We reported previously that transcription of pancRNAs from pBiPs epigenetically activates partner tissue-specific genes (7,8,11). Consistent with previous reports that pancRNAs contribute to the establishment of cell identity via epigenetic regulation of tissue-specific gene expression, the expression levels of pancRNAs derived from pBiPs tended to be positively correlated with the expression levels of their partner mRNAs during differentiation of PC12 cells (Figure 3C). Furthermore, epigenetic activation via pancRNAs was confirmed here by the manipulation of the *pancNusap1* levels in PC12 cells (Figures 5–7). Thus, the present results provide the new insight that transcriptional regulation by means of pancRNAs provides adaptive advantages for CRE-mediated gene regulation. Considering that the number of pBiPs is almost 6-fold greater than the number of aBiPs, the impacts of pBiPs as important effectors of cAMP signals might be greater than those of aBiPs for coordinated activation of a fraction of cAMP-responsive genes.

The silencing of M-phase progression contributes to the establishment of an irreversibly differentiated state: implications for neuronal differentiation

We showed that regulation of cell-cycle-associated genes plays crucial roles in the process of irreversible differentiation of PC12 cells (Figures 5–7). The critical importance of maintaining the cell-cycle-arrested state in neurons is supported by studies on somatic cell nuclear transfer. When nuclei of adult cortical neurons are used as donors, the majority of reconstructed mouse oocytes are arrested at the first mitotic cleavage with abnormal chromosome condensation (40), whereas reconstructed oocytes cloned from nuclei of other types of differentiated somatic cells, such as cumulus cells (41) and tail tip fibroblasts (42), show much greater developmental potential. Because the cell cycle of neurons is arrested at G0 phase, many studies have focused on the relationship between neuronal differentiation and inhibition of G1/S-phase progression (43,44). For example, neuronal differentiation of mouse neural stem cells is enhanced by double knockout of G1/S-phase-progression-associated genes *Cdk2* and *Cdk4* (45). Similarly, Ndiff PC12 cells have been widely used as an *in vitro* model for investigating the relationship between G1/S-phase inhibition and neurite outgrowth. In fact, like the Cdk2 protein level, the level of Pcna and phosphorylated retinoblastoma protein, also known as G1/S-phase-progression-associated proteins, are downregulated in Ndiff PC12 cells (46–48), suggesting that G1/S-phase inhibition also occurs in reversibly differentiated Ndiff PC12 cells.

In addition, several lines of evidence indicate that inhibition of M-phase-associated genes is involved in the functional differentiation of neurons (49,50). For example, reconstructed mouse oocytes cloned from nuclei of adult cortical neurons undergo abnormal cell cycle arrest at the first mitotic cleavage (40). In mouse neural progenitors, KD of an M-phase-progression-associated gene, doublecortin-like kinase, causes neuronal differentiation (51). Therefore, coordinated regulation of G1/S-phase-progression-associated genes and M-phase-progression-associated genes seems to be important for neuronal differentiation. In this context, it is interesting to note that the expression of cell-cycle-associated genes, especially those related to G2/M-phase progression, remained high in Ndiff PC12 cells (Figure 2) and epigenetic silencing of M-phase-associated *Nusap1* could convert reversibly differentiated cells into irreversibly differentiated cells (Figure 5). Considering that inhibition of G1/S-phase progression is observed in reversibly differentiated Ndiff PC12 cells (Supplementary Figure S14), NGF and cAMP signalings appear to be strongly involved in G1/S- and G2/M-inhibition, respectively, for completing the differentiation of neurons. Our results suggested that irreversible/reversible PC12 differentiation could be a good model for further addressing the lncRNA-mediated mechanisms that link cell cycle regulation to irreversible differentiation.

The pancRNA repertoires are differentially utilized from the zygotic to the terminally differentiated stages

In this study, the RNA-seq method was utilized to test whether pancRNA-mediated gene activation mechanisms function in the terminal differentiation of the cells on a genome-wide scale, and the results confirmed this hypothesis (Figures 3, 5 and 6). Indeed, pancRNAs have been detected from more than a thousand promoter regions at a very early stage of life called zygotic gene activation (7). Previous reports have also shown that thousands of pancRNAs are transcribed in ES cells and various tissues (11,52). Thus, a non-negligible number of pancRNAs seem to be expressed in various contexts. Since pancRNAs and mRNAs exhibit coordinated expression changes not only in totipotent/pluripotent cells but also in terminally differentiated cells (Figure 3C), pancRNAs may be commonly utilized for gene activation from the zygotic to the terminally differentiated stage. Although we focused on a study of functional pancRNAs from the polyA+ and >200 bp ncRNA fraction in this study, other fractions of ncRNAs (e.g. polyA-, <200 bp) derived from the promoter of protein-coding genes may also function in transcriptional activation of their partner genes (37,53). The general usage of the pancRNA system over the course of life sheds light on the importance of gene-activation-associated ncRNAs as counterparts of gene-silencing ncRNAs, such as microRNA, which work at the post-transcriptional level. Studies of possible coordinated regulation with lncRNAs derived from enhancer regions, called eRNAs (32,54–59) would be the next step in elucidating the sequence-specific gene activation mechanisms in which ncRNA structurally recognizes genomic DNA.

Transcriptional silencing of *Nusap1* in response to extracellular differentiation stimuli is an important step of cAMP signaling toward terminal differentiation of PC12 cells

Nusap1 protein has a well-conserved microtubule-binding domain in its COOH terminus and a DNA-binding SAP domain in its NH2 terminus, and promotes the stabilization and crosslinking of microtubules near chromosomes

in metaphase/anaphase (60,61). *Nusap1* is highly expressed in proliferative tissues, and essential for M-phase progression. In cultured cell lines, KD of *Nusap1* causes severe mitotic defects with defective anaphase and cytokinesis (60), and knockout of *Nusap1* induces early embryonic lethality in mice (62). Like other cell cycle regulators, the protein level of Nusap1 is under the regulation of a multisubunit E3 ubiquitin ligase, anaphase promoting complex/cyclosome, in proliferating cells (63). However, the mechanisms of transcriptional regulation of *Nusap1* in terminally differentiated cells are still unknown. In this study, we showed that reduced transcription of *Nusap1* via downregulation of *pancNusap1* in response to cAMP stimulation functions in the terminal differentiation of PC12 cells (Figures 5–8). These findings indicated that transcriptional silencing of *Nusap1* is a key mediator of cAMP signaling for terminal differentiation of PC12 cells. The epigenetic silencing by the concomitant reduction of *pancNusap1* by cAMP may further support the complete shut-down of neuronal cell division.

Possible molecular mechanism underlying *pancNusap1*-mediated epigenetic modification

We and others have reported that pancRNA promotes the assembly of an open chromatin conformation that includes histone acetylation, H3K4 methylation, H3K9/K27 demethylation and active DNA demethylation (7,8,12,64). Differently from these previous results, the present data indicated that the activation and reduction of *pancNusap1* expression increased and decreased the histone acetylation levels of the *Nusap1* promoter, respectively, but not the levels of histone methylation or DNA methylation (Figures 4–6, and Supplementary Figure S1). There are many reports indicating that functional lncRNAs recruit epigenetic modification complexes, such as histone methyltransferase myeloid/lymphoid or mixed-lineage leukemia (MLL) complex and the BER components at specific genomic locations (1,56,65–67). However there are no reports that prove the interaction of lncRNAs with histone acetyltransferase complex. Recently, nuclease-null Cas9-based transcriptional activation technology has revealed that artificial transcription initiation at an intergenic locus elevates H3K27ac levels (68). Furthermore, single living cell analysis has shown that recruitment of RNAPII occurs within a few minutes after histone acetylation at the glucocorticoid receptor gene locus (69). Given these reports, one possible scenario is that transcription initiation of *pancNusap1* primary causes histone acetylation at the *Nusap1* promoter and thus enhances specific gene expression there.

Interestingly, we and others have reported that only antisense pancRNAs are associated with chromatin, and pancRNA-mediated transcriptional activation occurs in a strand-specific manner (8,64). Consistent with these reports, the transcriptional direction of *pancNusap1* is important for *pancNusap1*-mediated histone acetylation (Figure 6). In this context, it is worthwhile to note that *pancNusap1* has a G-rich sequence (Supplementary Figure S15). Because guanine (G)-rich RNA that hybridizes with single-stranded cytosine (C)-rich complementary DNA forms a thermodynamically stable DNA:RNA hybrid structure, known as an R-loop structure (70,71), the sequence-dependent stability of R-loops may explain the increase of histone acetylation by *pancNusap1*. Further studies will be needed to unravel the molecular mechanisms that determine the sequential epigenetic changes induced by pancRNA-mediated histone acetylation.

In conclusion, pancRNA-mediated histone acetylation contributes to the establishment of PC12 cells' stimulation-induced transcription status during the irreversible differentiation process.

DATA AVAILABILITY

RNA-seq data have been deposited in the DDBJ Sequence Read Archive (DRA) under accession number DRA004148.

SUPPLEMENTARY DATA

Supplementary Data are available at NAR Online.

ACKNOWLEDGEMENT

We thank Osamu Nishimura and Masahiro Uesaka for providing advice about transcriptome analysis; Nobuhiko Hamazaki and Hirofumi Noguchi for scientific insights and suggestions throughout the study; Katsuhide Igarashi, Hideyuki Nakashima, Tsukasa Sanosaka and Sayako Katada for experimental advice; and Elizabeth Nakajima for proofreading the manuscript.

FUNDING

Japan Society for the Promotion of Science [15H04603; 24380158 to T. I., 241544 to N. Y.]; Global COE program [A06 to Kyoto University]; Scientific Research on Innovative Areas 'Genome Science' from the Ministry of Education, Culture, Sports, Science and Technology (MEXT) [221S0002 to T.I.]. Funding for open access charge: Japan Society for the Promotion of Science [15H04603, 24380158 to T. I., 241544 to N. Y.]; Global COE program [A06 to Kyoto University]; Scientific Research on Innovative Areas 'Genome Science' from the Ministry of Education, Culture, Sports, Science and Technology (MEXT) [221S0002].
Conflict of interest statement. None declared.

REFERENCES

1. Guttman,M., Donaghey,J., Carey,B.W., Garber,M., Grenier,J.K., Munson,G., Young,G., Lucas,A.B., Ach,R., Bruhn,L. *et al.* (2011) lincRNAs act in the circuitry controlling pluripotency and differentiation. *Nature*, **477**, 295–300.
2. Carrieri,C., Cimatti,L., Biagioli,M., Beugnet,A., Zucchelli,S., Fedele,S., Pesce,E., Ferrer,I., Collavin,L., Santoro,C. *et al.* (2012) Long non-coding antisense RNA controls Uchl1 translation through an embedded SINEB2 repeat. *Nature*, **491**, 454–457.
3. Ng,S.-Y., Bogu,G.K., Soh,B.S. and Stanton,L.W. (2013) The long noncoding RNA RMST interacts with SOX2 to regulate neurogenesis. *Mol. Cell*, **51**, 349–359.
4. Herzog,V.A., Lempradl,A., Trupke,J., Okulski,H., Altmutter,C., Ruge,F., Boidol,B., Kubicek,S., Schmauss,G., Aumayr,K. *et al.* (2014) A strand-specific switch in noncoding transcription switches the function of a Polycomb/Trithorax response element. *Nat. Genet.*, **46**, 973–981.

5. Ting,A.H., Schuebel,K.E., Herman,J.G. and Baylin,S.B. (2005) Short double-stranded RNA induces transcriptional gene silencing in human cancer cells in the absence of DNA methylation. *Nat. Genet.*, **37**, 906–910.
6. Gupta,R.A., Shah,N., Wang,K.C., Kim,J., Horlings,H.M., Wong,D.J., Tsai,M.-C., Hung,T., Argani,P., Rinn,J.L. *et al.* (2010) Long non-coding RNA HOTAIR reprograms chromatin state to promote cancer metastasis. *Nature*, **464**, 1071–1076.
7. Hamazaki,N., Uesaka,M., Nakashima,K., Agata,K. and Imamura,T. (2015) Gene activation-associated long noncoding RNAs function in mouse preimplantation development. *Development*, **142**, 910–920.
8. Tomikawa,J., Shimokawa,H., Uesaka,M., Yamamoto,N., Mori,Y., Tsukamura,H., Maeda,K.-I. and Imamura,T. (2011) Single-stranded noncoding RNAs mediate local epigenetic alterations at gene promoters in rat cell lines. *J. Biol. Chem.*, **286**, 34788–34799.
9. Sigova,A.A., Abraham,B.J., Ji,X., Molinie,B., Hannett,N.M., Guo,Y.E., Jangi,M., Giallourakis,C.C., Sharp,P.A. and Young,R.A. (2015) Transcription factor trapping by RNA in gene regulatory elements. *Science*, **350**, 978–981.
10. Ravasi,T., Suzuki,H., Pang,K.C., Katayama,S., Furuno,M., Okunishi,R., Fukuda,S., Ru,K., Frith,M.C., Gongora,M.M. *et al.* (2006) Experimental validation of the regulated expression of large numbers of non-coding RNAs from the mouse genome. *Genome Res.*, **16**, 11–19.
11. Uesaka,M., Nishimura,O., Go,Y., Nakashima,K., Agata,K. and Imamura,T. (2014) Bidirectional promoters are the major source of gene activation-associated non-coding RNAs in mammals. *BMC Genomics*, **15**, 35.
12. Imamura,T., Yamamoto,S., Ohgane,J., Hattori,N., Tanaka,S. and Shiota,K. (2004) Non-coding RNA directed DNA demethylation of Sphk1 CpG island. *Biochem. Biophys. Res. Commun.*, **322**, 593–600.
13. Hegedus,B., Dasgupta,B., Shin,J.E., Emnett,R.J., Hart-Mahon,E.K., Elghazi,L., Bernal-Mizrachi,E. and Gutmann,D.H. (2007) Neurofibromatosis-1 regulates neuronal and glial cell differentiation from neuroglial progenitors in vivo by both cAMP- and Ras-dependent mechanisms. *Cell Stem Cell*, **1**, 443–457.
14. Zahir,T., Chen,Y.F., MacDonald,J.F., Leipzig,N., Tator,C.H. and Shoichet,M.S. (2009) Neural stem/progenitor cells differentiate in vitro to neurons by the combined action of dibutyryl cAMP and interferon-gamma. *Stem Cells Dev.*, **18**, 1423–1432.
15. Impey,S., McCorkle,S.R., Cha-Molstad,H., Dwyer,J.M., Yochum,G.S., Boss,J.M., McWeeney,S., Dunn,J.J., Mandel,G. and Goodman,R.H. (2004) Defining the CREB regulon: a genome-wide analysis of transcription factor regulatory regions. *Cell*, **119**, 1041–1054.
16. Cha-Molstad,H., Keller,D.M., Yochum,G.S., Impey,S. and Goodman,R.H. (2004) Cell-type-specific binding of the transcription factor CREB to the cAMP-response element. *Proc. Natl. Acad. Sci. U.S.A.*, **101**, 13572–13577.
17. Molina,C.A., Foulkes,N.S., Lalli,E. and Sassone-Corsi,P. (1993) Inducibility and negative autoregulation of CREM: an alternative promoter directs the expression of ICER, an early response repressor. *Cell*, **75**, 875–886.
18. Klejman,A. and Kaczmarek,L. (2006) Inducible cAMP early repressor (ICER) isoforms and neuronal apoptosis in cortical in vitro culture. *Acta Neurobiol. Exp. (Wars)*, **66**, 267–272.
19. Borlikova,G. and Endo,S. (2009) Inducible cAMP early repressor (ICER) and brain functions. *Mol. Neurobiol.*, **40**, 73–86.
20. Okoshi,R., Kubo,N., Nakashima,K., Shimozato,O., Nakagawara,A. and Ozaki,T. (2011) CREB represses p53-dependent transactivation of MDM2 through the complex formation with p53 and contributes to p53-mediated apoptosis in response to glucose deprivation. *Biochem. Biophys. Res. Commun.*, **406**, 79–84.
21. Gunning,P.W., Landreth,G.E., Layer,P., Ignatius,M. and Shooter,E.M. (1981) Nerve growth factor-induced differentiation of PC12 cells: evaluation of changes in RNA and DNA metabolism. *J. Neurosci.*, **1**, 368–379.
22. Michel,P.P., Vyas,S. and Agid,Y. (1995) Synergistic differentiation by chronic exposure to cyclic AMP and nerve growth factor renders rat phaeochromocytoma PC12 cells totally dependent upon trophic support for survival. *Eur. J. Neurosci.*, **7**, 251–260.
23. Kim,D., Pertea,G., Trapnell,C., Pimentel,H., Kelley,R. and Salzberg,S.L. (2013) TopHat2: accurate alignment of transcriptomes in the presence of insertions, deletions and gene fusions. *Genome Biol.*, **14**, R36.
24. Wang,L., Wang,S. and Li,W. (2012) RSeQC: quality control of RNA-seq experiments. *Bioinformatics*, **28**, 2184–2185.
25. Zhang,Y., Liu,T., Meyer,C.A., Eeckhoute,J., Johnson,D.S., Bernstein,B.E., Nusbaum,C., Myers,R.M., Brown,M., Li,W. *et al.* (2008) Model-based analysis of ChIP-Seq (MACS). *Genome Biol.*, **9**, R137.
26. Quinlan,A.R. and Hall,I.M. (2010) BEDTools: a flexible suite of utilities for comparing genomic features. *Bioinformatics*, **26**, 841–842.
27. Kong,L., Zhang,Y., Ye,Z.-Q., Liu,X.-Q., Zhao,S.-Q., Wei,L. and Gao,G. (2007) CPC: assess the protein-coding potential of transcripts using sequence features and support vector machine. *Nucleic Acids Res.*, **35**, W345–W349.
28. Sun,J., Nishiyama,T., Shimizu,K. and Kadota,K. (2013) TCC: an R package for comparing tag count data with robust normalization strategies. *BMC Bioinformatics*, **14**, 219.
29. Huang,D.W., Sherman,B.T. and Lempicki,R.A. (2009) Systematic and integrative analysis of large gene lists using DAVID bioinformatics resources. *Nat Protoc*, **4**, 44–57.
30. Zhu,L.J., Gazin,C., Lawson,N.D., Pagès,H., Lin,S.M., Lapointe,D.S. and Green,M.R. (2010) ChIPpeakAnno: a bioconductor package to annotate ChIP-seq and ChIP-chip data. *BMC Bioinformatics*, **11**, 237.
31. Mathelier,A., Zhao,X., Zhang,A.W., Parcy,F., Worsley-Hunt,R., Arenillas,D.J., Buchman,S., Chen,C.-Y., Chou,A., Ienasescu,H. *et al.* (2014) JASPAR 2014: an extensively expanded and updated open-access database of transcription factor binding profiles. *Nucleic Acids Res.*, **42**, D142–D147.
32. Kim,T.-K., Hemberg,M., Gray,J.M., Costa,A.M., Bear,D.M., Wu,J., Harmin,D.A., Laptewicz,M., Barbara-Haley,K., Kuersten,S. *et al.* (2010) Widespread transcription at neuronal activity-regulated enhancers. *Nature*, **465**, 182–187.
33. Lesiak,A., Pelz,C., Ando,H., Zhu,M., Davare,M., Lambert,T.J., Hansen,K.F., Obrietan,K., Appleyard,S.M., Impey,S. *et al.* (2013) A genome-wide screen of CREB occupancy identifies the RhoA inhibitors Par6C and Rnd3 as regulators of BDNF-induced synaptogenesis. *PLoS One*, **8**, e64658.
34. La Rocca,R., Fulciniti,M., Lakshmikanth,T., Mesuraca,M., Ali,T.H., Mazzei,V., Amodio,N., Catalano,L., Rotoli,B., Ouerfelli,O. *et al.* (2009) Early hematopoietic zinc finger protein prevents tumor cell recognition by natural killer cells. *J. Immunol.*, **182**, 4529–4537.
35. Shin,K.-J., Wall,E.A., Zavzavadjian,J.R., Santat,L.A., Liu,J., Hwang,J.-I., Rebres,R., Roach,T., Seaman,W., Simon,M.I. *et al.* (2006) A single lentiviral vector platform for microRNA-based conditional RNA interference and coordinated transgene expression. *Proc. Natl. Acad. Sci. U.S.A.*, **103**, 13759–13764.
36. Zufferey,R., Dull,T., Mandel,R.J., Bukovsky,A., Quiroz,D., Naldini,L. and Trono,D. (1998) Self-inactivating lentivirus vector for safe and efficient in vivo gene delivery. *J. Virol.*, **72**, 9873–9880.
37. Seila,A.C., Calabrese,J.M., Levine,S.S., Yeo,G.W., Rahl,P.B., Flynn,R.A., Young,R.A. and Sharp,P.A. (2008) Divergent transcription from active promoters. *Science*, **322**, 1849–1851.
38. Hu,H.Y., He,L. and Khaitovich,P. (2014) Deep sequencing reveals a novel class of bidirectional promoters associated with neuronal genes. *BMC Genomics*, **15**, 457.
39. Chang,J.H., Vuppalanchi,D., van Niekerk,E., Trepel,J.B., Schanen,N.C. and Twiss,J.L. (2006) PC12 cells regulate inducible cyclic AMP (cAMP) element repressor expression to differentially control cAMP response element-dependent transcription in response to nerve growth factor and cAMP. *J. Neurochem.*, **99**, 1517–1530.
40. Osada,T., Kusakabe,H., Akutsu,H., Yagi,T. and Yanagimachi,R. (2002) Adult murine neurons: their chromatin and chromosome changes and failure to support embryonic development as revealed by nuclear transfer. *Cytogenet. Genome Res.*, **97**, 7–12.
41. Wakayama,T., Perry,A.C., Zuccotti,M., Johnson,K.R. and Yanagimachi,R. (1998) Full-term development of mice from enucleated oocytes injected with cumulus cell nuclei. *Nature*, **394**, 369–374.
42. Wakayama,T. and Yanagimachi,R. (1999) Cloning of male mice from adult tail-tip cells. *Nat. Genet.*, **22**, 127–128.
43. Lee,E.Y., Hu,N., Yuan,S.S., Cox,L.A., Bradley,A., Lee,W.H. and Herrup,K. (1994) Dual roles of the retinoblastoma protein in cell cycle regulation and neuron differentiation. *Genes Dev.*, **8**, 2008–2021.

44. Galderisi,U., Jori,F.P. and Giordano,A. (2003) Cell cycle regulation and neural differentiation. *Oncogene*, **22**, 5208–5219.
45. Lim,S. and Kaldis,P. (2012) Loss of Cdk2 and Cdk4 induces a switch from proliferation to differentiation in neural stem cells. *Stem Cells*, **30**, 1509–1520.
46. Yan,G.Z. and Ziff,E.B. (1995) NGF regulates the PC12 cell cycle machinery through specific inhibition of the Cdk kinases and induction of cyclin D1. *J. Neurosci.*, **15**, 6200–6212.
47. Yan,G.Z. and Ziff,E.B. (1997) Nerve growth factor induces transcription of the p21 WAF1/CIP1 and cyclin D1 genes in PC12 cells by activating the Sp1 transcription factor. *J. Neurosci.*, **17**, 6122–6132.
48. Dobashi,Y., Shoji,M., Kitagawa,M., Noguchi,T. and Kameya,T. (2000) Simultaneous suppression of cdc2 and cdk2 activities induces neuronal differentiation of PC12 cells. *J. Biol. Chem.*, **275**, 12572–12580.
49. Hayes,T.E., Valtz,N.L. and McKay,R.D. (1991) Downregulation of CDC2 upon terminal differentiation of neurons. *New Biol.*, **3**, 259–269.
50. Okano,H.J., Pfaff,D.W. and Gibbs,R.B. (1993) RB and Cdc2 expression in brain: correlations with 3H-thymidine incorporation and neurogenesis. *J. Neurosci.*, **13**, 2930–2938.
51. Shu,T., Tseng,H.-C., Sapir,T., Stern,P., Zhou,Y., Sanada,K., Fischer,A., Coquelle,F.M., Reiner,O. and Tsai,L.-H. (2006) Doublecortin-like kinase controls neurogenesis by regulating mitotic spindles and M phase progression. *Neuron*, **49**, 25–39.
52. Sigova,A.A., Mullen,A.C., Molinie,B., Gupta,S., Orlando,D.A., Guenther,M.G., Almada,A.E., Lin,C., Sharp,P.A., Giallourakis,C.C. *et al.* (2013) Divergent transcription of long noncoding RNA/mRNA gene pairs in embryonic stem cells. *Proc. Natl. Acad. Sci. U.S.A.*, **110**, 2876–2881.
53. Kapranov,P., Cheng,J., Dike,S., Nix,D.A., Duttagupta,R., Willingham,A.T., Stadler,P.F., Hertel,J., Hackermüller,J., Hofacker,I.L. *et al.* (2007) RNA maps reveal new RNA classes and a possible function for pervasive transcription. *Science*, **316**, 1484–1488.
54. Melgar,M.F., Collins,F.S. and Sethupathy,P. (2011) Discovery of active enhancers through bidirectional expression of short transcripts. *Genome Biol.*, **12**, R113.
55. Hah,N., Murakami,S., Nagari,A., Danko,C.G. and Kraus,W.L. (2013) Enhancer transcripts mark active estrogen receptor binding sites. *Genome Res.*, **23**, 1210–1223.
56. Kaikkonen,M.U., Spann,N.J., Heinz,S., Romanoski,C.E., Allison,K.A., Stender,J.D., Chun,H.B., Tough,D.F., Prinjha,R.K., Benner,C. *et al.* (2013) Remodeling of the enhancer landscape during macrophage activation is coupled to enhancer transcription. *Mol. Cell*, **51**, 310–325.
57. Lai,F., Orom,U.A., Cesaroni,M., Beringer,M., Taatjes,D.J., Blobel,G.A. and Shiekhattar,R. (2013) Activating RNAs associate with Mediator to enhance chromatin architecture and transcription. *Nature*, **494**, 497–501.
58. Andersson,R., Gebhard,C., Miguel-Escalada,I., Hoof,I., Bornholdt,J., Boyd,M., Chen,Y., Zhao,X., Schmidl,C., Suzuki,T. *et al.* (2014) An atlas of active enhancers across human cell types and tissues. *Nature*, **507**, 455–461.
59. Léveillé,N., Melo,C.A., Rooijers,K., Díaz-Lagares,A., Melo,S.A., Korkmaz,G., Lopes,R., Akbari Moqadam,F., Maia,A.R., Wijchers,P.J. *et al.* (2015) Genome-wide profiling of p53-regulated enhancer RNAs uncovers a subset of enhancers controlled by a lncRNA. *Nat. Commun.*, **6**, 6520.
60. Raemaekers,T., Ribbeck,K., Beaudouin,J., Annaert,W., Van Camp,M., Stockmans,I., Smets,N., Bouillon,R., Ellenberg,J. and Carmeliet,G. (2003) NuSAP, a novel microtubule-associated protein involved in mitotic spindle organization. *J. Cell Biol.*, **162**, 1017–1029.
61. Ribbeck,K., Raemaekers,T., Carmeliet,G. and Mattaj,I.W. (2007) A role for NuSAP in linking microtubules to mitotic chromosomes. *Curr. Biol.*, **17**, 230–236.
62. Vanden Bosch,A., Raemaekers,T., Denayer,S., Torrekens,S., Smets,N., Moermans,K., Dewerchin,M., Carmeliet,P. and Carmeliet,G. (2010) NuSAP is essential for chromatin-induced spindle formation during early embryogenesis. *J. Cell. Sci.*, **123**, 3244–3255.
63. Li,L., Zhou,Y., Sun,L., Xing,G., Tian,C., Sun,J., Zhang,L. and He,F. (2007) NuSAP is degraded by APC/C-Cdh1 and its overexpression results in mitotic arrest dependent of its microtubules' affinity. *Cell. Signal.*, **19**, 2046–2055.
64. Boque-Sastre,R., Soler,M., Oliveira-Mateos,C., Portela,A., Moutinho,C., Sayols,S., Villanueva,A., Esteller,M. and Guil,S. (2015) Head-to-head antisense transcription and R-loop formation promotes transcriptional activation. *Proc. Natl. Acad. Sci. U.S.A.*, **112**, 5785–5790.
65. Wang,K.C., Yang,Y.W., Liu,B., Sanyal,A., Corces-Zimmerman,R., Chen,Y., Lajoie,B.R., Protacio,A., Flynn,R.A., Gupta,R.A. *et al.* (2011) A long noncoding RNA maintains active chromatin to coordinate homeotic gene expression. *Nature*, **472**, 120–124.
66. Yang,L., Lin,C., Jin,C., Yang,J.C., Tanasa,B., Li,W., Merkurjev,D., Ohgi,K.A., Meng,D., Zhang,J. *et al.* (2013) lncRNA-dependent mechanisms of androgen-receptor-regulated gene activation programs. *Nature*, **500**, 598–602.
67. Puc,J., Kozbial,P., Li,W., Tan,Y., Liu,Z., Suter,T., Ohgi,K.A., Zhang,J., Aggarwal,A.K. and Rosenfeld,M.G. (2015) Ligand-dependent enhancer activation regulated by topoisomerase-I activity. *Cell*, **160**, 367–380.
68. Hilton,I.B., D'Ippolito,A.M., Vockley,C.M., Thakore,P.I., Crawford,G.E., Reddy,T.E. and Gersbach,C.A. (2015) Epigenome editing by a CRISPR-Cas9-based acetyltransferase activates genes from promoters and enhancers. *Nat. Biotechnol.*, **33**, 510–517.
69. Stasevich,T.J., Hayashi-Takanaka,Y., Sato,Y., Maehara,K., Ohkawa,Y., Sakata-Sogawa,K., Tokunaga,M., Nagase,T., Nozaki,N., McNally,J.G. *et al.* (2014) Regulation of RNA polymerase II activation by histone acetylation in single living cells. *Nature*, **516**, 272–275.
70. Ratmeyer,L., Vinayak,R., Zhong,Y.Y., Zon,G. and Wilson,W.D. (1994) Sequence specific thermodynamic and structural properties for DNA.RNA duplexes. *Biochemistry*, **33**, 5298–5304.
71. Roberts,R.W. and Crothers,D.M. (1992) Stability and properties of double and triple helices: dramatic effects of RNA or DNA backbone composition. *Science*, **258**, 1463–1466.